Article

Cell Reports

Endothelial Cells in the Decidual Bed Are Potential Therapeutic Targets for Preterm Birth Prevention

Graphical Abstract

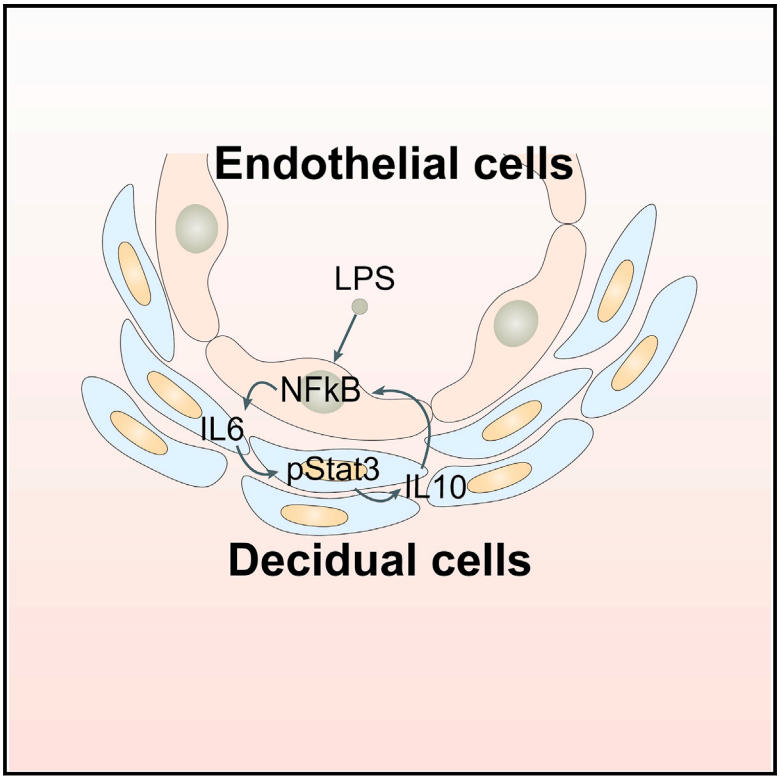

Authors

Wenbo Deng, Jia Yuan, Jeeyeon Cha, ..., Hideo Yagita, Yasushi Hirota, Sudhansu K. Dey

Correspondence

sk.dey@cchmc.org

In Brief

Deng et al. show a balance between inflammation and anti-inflammation involving endothelial and decidual cells in pregnancy. Tipping this balance toward inflammation contributes to preterm birth. A mechanism to preserve homeostatic balance in pregnancy under inflammation is mediated by a cross-talk between endothelial and perivascular stromal cells.

Highlights

- Endothelial TLR4-mediated inflammation in the decidual bed contributes to preterm birth
- Endothelial-stromal cell cross-talk confers a homeostatic balance in pregnant uteri
- TLR4-Stat3 signaling regulates anti-inflammatory IL-10 expression to protect pregnancy
- Tipping the balance toward inflammation induces preterm birth

Deng et al., 2019, Cell Reports *27*, 1755–1768
May 7, 2019
https://doi.org/10.1016/j.celrep.2019.04.049

CellPress

Cell Reports
Article

Endothelial Cells in the Decidual Bed Are Potential Therapeutic Targets for Preterm Birth Prevention

Wenbo Deng,[1,2,6] Jia Yuan,[1,2,6] Jeeyeon Cha,[3] Xiaofei Sun,[1,2] Amanda Bartos,[1,2] Hideo Yagita,[4] Yasushi Hirota,[5] and Sudhansu K. Dey[1,2,7,*]

[1]Division of Reproductive Sciences, Cincinnati Children's Hospital Medical Center, Cincinnati, OH 45299, USA
[2]College of Medicine, University of Cincinnati, Cincinnati, OH 45221, USA
[3]Division of Diabetes, Endocrinology, and Metabolism, Department of Internal Medicine, Vanderbilt University Medical Center, Nashville, TN 37232, USA
[4]Department of Immunology, Juntendo University School of Medicine, 2-1-1 Hongo, Bunkyo-ku, Tokyo 113-8421, Japan
[5]Department of Obstetrics and Gynecology, University of Tokyo, Japan
[6]These authors contributed equally
[7]Lead Contact
*Correspondence: sk.dey@cchmc.org
https://doi.org/10.1016/j.celrep.2019.04.049

SUMMARY

Preterm birth (PTB) is a syndrome with many origins. Among them, infection or inflammation are major risk factors for PTB; however, local defense mechanisms to mount anti-inflammatory responses against inflammation-induced PTB are poorly understood. Here, we show that endothelial TLR4 in the decidual bed is critical for sensing inflammation during pregnancy because mice with endothelial *Tlr4* deletion are resistant to lipopolysaccharide (LPS)-induced PTB. Under inflammatory conditions, IL-6 is readily expressed in decidual endothelial cells with signal transducer and activator of transcription 3 (Stat3) phosphorylation in perivascular stromal cells, which then regulates expression of anti-inflammatory IL-10. Our observation that administration of an IL-10 neutralizing antibody predisposing mice to PTB shows IL-10's anti-inflammatory role to prevent PTB. We show that the integration of endothelial and perivascular stromal signaling can determine pregnancy outcomes. These findings highlight a role for endothelial TLR4 in inflammation-induced PTB and may offer a potential therapeutic target to prevent PTB.

INTRODUCTION

Preterm birth (PTB) is a leading cause of child mortality and morbidity and often incurs life-long clinical and psychological challenges for the survivors (Moster et al., 2008). Many risk factors, including genetic predisposition, bacterial infection or inflammation, maternal aging, hormonal imbalances, and environmental stresses, contribute toward this complex pathology (Goldenberg et al., 2008; Romero et al., 2014). PTB can result from both systemic and local inflammation in the reproductive tract and/or feto-placental unit (Elovitz and Mrinalini, 2004). The mechanism underlying PTB remains intangible, especially in humans due to logistical and ethical difficulties in accessing meaningful samples. Suitable animal models to recapitulate the human conditions are alternative viable options. Genetic and/or experimentally manipulated mouse models predisposed to PTB can mimic certain aspects of PTB in humans (Cha et al., 2013). In this context, mouse models can provide the advantage of studying gene-environment influences on PTB in a defined set of experimental and dietary conditions as opposed to human tissue analyses obtained from placentas under diverse settings. Genetic mouse models can also offer opportunities to explore the interplay between inflammatory and anti-inflammatory pathways in PTB. The availability of a sufficient number of placentas from diverse groups with different ethnic backgrounds with different food habits, living conditions, and environment may be limiting factors to provide meaningful results. The scenario is more challenging for the socioeconomically depressed population groups, which often show higher rate of PTB. Because PTB is a disorder with many origins (Romero et al., 2014), studies in both animal models and humans will provide more meaningful results that could be relevant to humans and other species.

Both the maternal decidua and feto-placental unit are thought to participate in PTB in response to infection or inflammation. However, whether causes of PTB originate from the decidua, placenta, and/or fetus has not been clearly distinguished. The maternal decidua serves as a "signaling hub" that coordinates interactions between the mother and feto-placental unit (Moffett and Loke, 2006). Effective reciprocal cross-talk between the decidua and feto-placental unit involving genetics, epigenetic modification, and transcription factors in combination with morphogens, cytokines, and signaling molecules creates a favorable milieu to support fetal growth and development and successful completion of pregnancy (Romero et al., 2014; Rubens et al., 2014). There is increasing interest in the decidua's role in

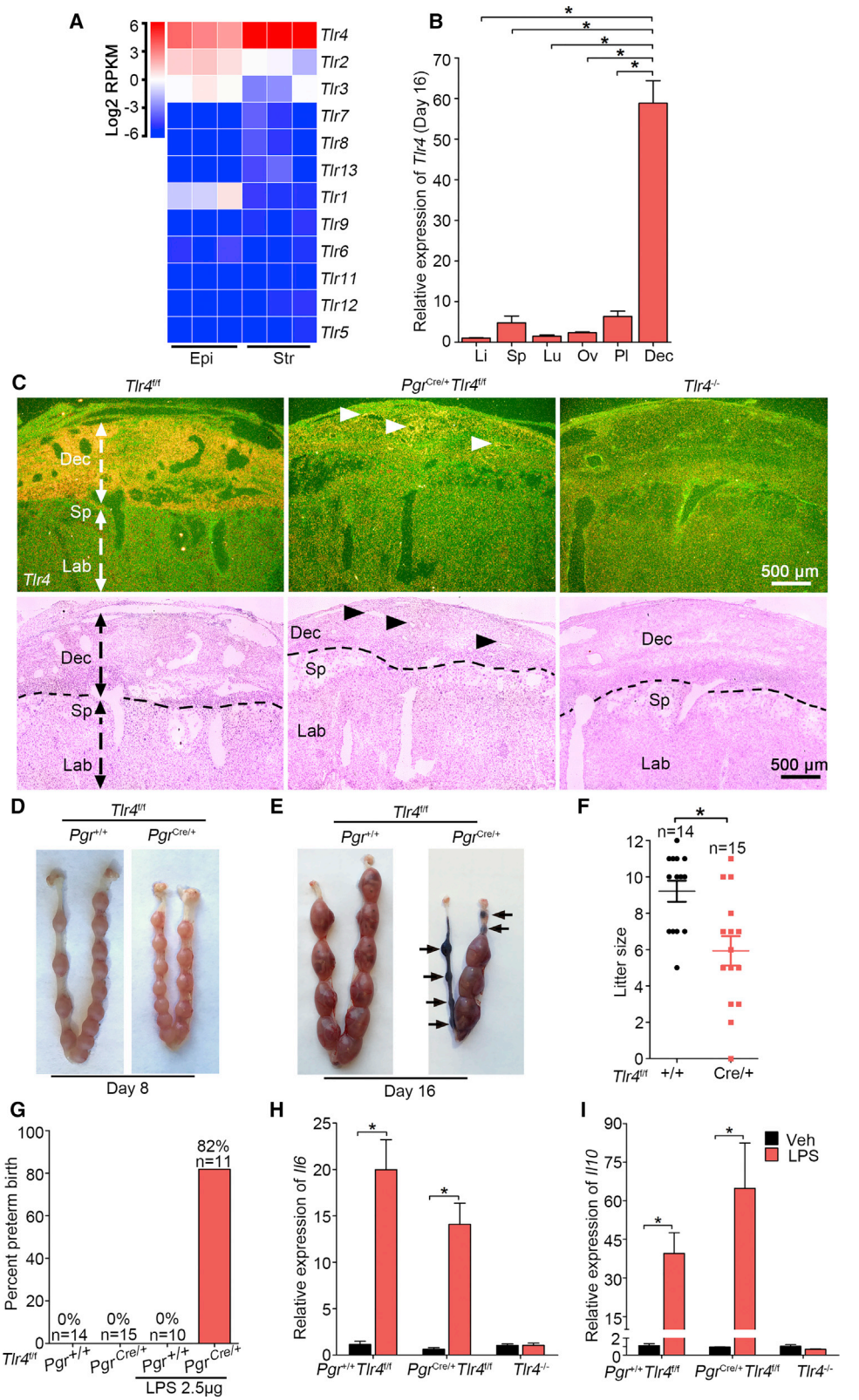

(legend on next page)

orchestrating the homeostatic balance between the mother and fetus, and studies suggest that the decidua is a critical regulator of birth timing and pregnancy well-being (Cha et al., 2013; Deng et al., 2016; Hirota et al., 2011; Hirota et al., 2010).

LPS, a gram-negative bacterial lipopolysaccharide, is a leading cause of inflammation through increased production of cytokines and chemokines. LPS primarily executes its function by Toll-like receptor 4 (TLR4) (Miller et al., 2005). Until now, the mechanism by which TLR4-induced inflammation induces PTB has largely been descriptive. There are reports that decidual macrophages and neutrophils express TLR4 and may play a role in inflammation-induced PTB (Kadam et al., 2017; Robertson et al., 2018; Yan et al., 2018); whether other TLR4-expressing cells are involved in inflammation-induced PTB remains unknown. Using genetic mouse models and breeding strategies, we sought to dissect the role of maternal decidua apart from the fetal-placental entity in response to systemic LPS injection. The uterus is comprised of heterogeneous tissues and cell types, and it is not known whether TLR4 expression and function are tissue- or cell-specific. Here, we explored the site of TLR4-mediated function in the uterus.

Using genetic and molecular approaches, we show that the decidua is a major site of expression of TLR4, which is sensitive to LPS exposure and release of cytokines. Further investigation found that decidual endothelial TLR4 is primarily responsible for rapid induction of pro-inflammatory cytokines if exposed to systemic LPS administration. This inflammatory insult initiates cross-talk between the decidual endothelial and perivascular stromal cells to mount a counter, anti-inflammatory response. Using conditional deletion of *Tlr4* in deciduae by a *Pgr-Cre* driver, we observed that dams with a loss of decidual *Tlr4* have reduced litter size and increased fetal resorption and they are highly sensitive to PTB by an ultra-low dose of LPS. We found that *Il6* is induced in endothelial cells by LPS and associated with activation of signal transducer and activator of transcription 3 (pStat3) in perivascular stromal cells; Stat3 activation is known to regulate *Il10* expression. Intriguingly, the deletion of endothelial *Tlr4* by a highly specific *Tie2-Cre* driver ($Tie2^{Cre/+}Tlr4^{f/f}$) shows resistance to even a high dose of LPS (40 μg/mouse) to PTB in these mice; this dose induces PTB in 100% of $Tlr4^{f/f}$ females. There is evidence that interleukin-6 (IL-6) induces anti-inflammatory IL-10 expression through pStat3 (Saraiva and O'Garra, 2010). Indeed, administration of IL-10-neutralizing antibodies predisposes mice to PTB if exposed to a very low dose of LPS. Collectively, our results show tissue-specific interactions and responses to inflammation to protect pregnancy against inflammatory insults. This study elucidates a role for endothelial TLR4 in calibrating proinflammatory versus anti-inflammatory responses in the decidua to determine the fate of pregnancy outcomes and inflammation-induced PTB in the context of LPS exposure and genetic predisposition.

RESULTS

Differential TLR4 Expression in the Decidua and Placenta

The uterus is comprised of heterogeneous tissue and cell types. LPS primarily executes its function by TLR4, leading to increased release of cytokines (Miller et al., 2005). It is not known if TLR4 function is tissue or cell type specific. TLRs belong to a large family, and our RNA sequencing (RNA-seq) data in isolated mouse epithelial and stromal cells show that *Tlr4* expression is highest among other members of the family in stromal cells (Figure 1A). More interestingly, *Tlr4* expression is much higher in day 16 deciduae than other organs, such as the liver, spleen, lung, ovary, and placenta (Figure 1B). The lower *Il10* expression in the placenta also suggests that the decidua is more active in anti-inflammatory responses (Figure S1A). As recently reported (Nancy et al., 2018), RNA-seq data in purified stromal cells on days 8 and 16 of pregnancy show highest *Tlr4* expression in deciduae, supporting our results and suggesting a potential role of TLR4 in the decidua (Figures S1B and S1C). Our *in situ* hybridization (ISH) results show that the expression of TLR4 is highly localized in day 16 deciduae with much lower expression in the placenta (Figure 1C), suggesting that the decidua is a potential site that modulates the balance between inflammation and anti-inflammation.

The above results prompted us to explore if TLR4 expression exhibits a similar pattern in humans. Indeed, TLR4 expression is highest among the family members in endometrial biopsies obtained from 20 healthy fertile women in the mid-secretory phase of the menstrual cycle, i.e., 8 days after luteinizing hormone peak (LH+8) (Figure S1D) (Altmäe et al., 2017). Another recent study that used single-cell RNA-seq analyses of first trimester deciduae and placentas shows that TLR4 expression is much higher in decidual stromal cells, decidual fibroblasts,

Figure 1. TLR4 Is Beneficial during Normal Pregnancy

(A) Heatmap of RNA-seq analysis of *Tlr* mRNAs (log2 RPKM) in separated epithelial (Epi) and stromal cells (Str) from day 4 pregnant uteri (n = 3). RPKM, reads per kilobase per million.

(B) Relative *Tlr4* expression levels in various organs in day 16 pregnant $Tlr4^{f/f}$ mice by qPCR. *rpL7* was used as internal controls. Li, liver; Sp, spleen; Lu, lung; Ov, ovary; Pl, placenta; Dec, decidua; n = 4, *p < 0.05. Data are represented as mean ± SEM.

(C) Dark-field and bright-field images of *in situ* hybridization for *Tlr4* in $Tlr4^{f/f}$, $Pgr^{Cre/+}Tlr4^{f/f}$, and *Tlr4* genomic knockout ($Tlr4^{-/-}$) mice. Arrow heads indicate remaining *Tlr4* in $Pgr^{Cre/+}Tlr4^{f/f}$ mice. Dotted lines demarcate the interface between maternal decidua and spongiotrophoblast. Dec, decidua; Sp, spongiotrophoblast; Lb, labyrinth. Scale bar, 500 μm.

(D and E) Days 8 (D) and 16 (E) implantation sites in $Tlr4^{f/f}$ and $Pgr^{Cre/+}Tlr4^{f/f}$ mice. Arrows indicate resorption sites.

(F) Live litter size in $Tlr4^{f/f}$ and $Pgr^{Cre/+}Tlr4^{f/f}$ mice. n, animal number in each group, *p < 0.05. Data are represented as mean ± SEM.

(G) The ratio of preterm birth to total number of pups per gestation in $Tlr4^{f/f}$ and $Pgr^{Cre/+}Tlr4^{f/f}$ mice with or without exposure to a low dose LPS (2.5 μg/mouse). n indicates the number of total mice examined in each group.

(H and I) qPCR of *Il6* (H) and *Il10* (I) mRNA levels in $Tlr4^{f/f}$, $Pgr^{Cre/+}Tlr4^{f/f}$, and $Tlr4^{-/-}$ mice after 1 h of LPS treatment. *p < 0.05. Data are represented as mean ± SEM (n = 4).

See also Figure S1.

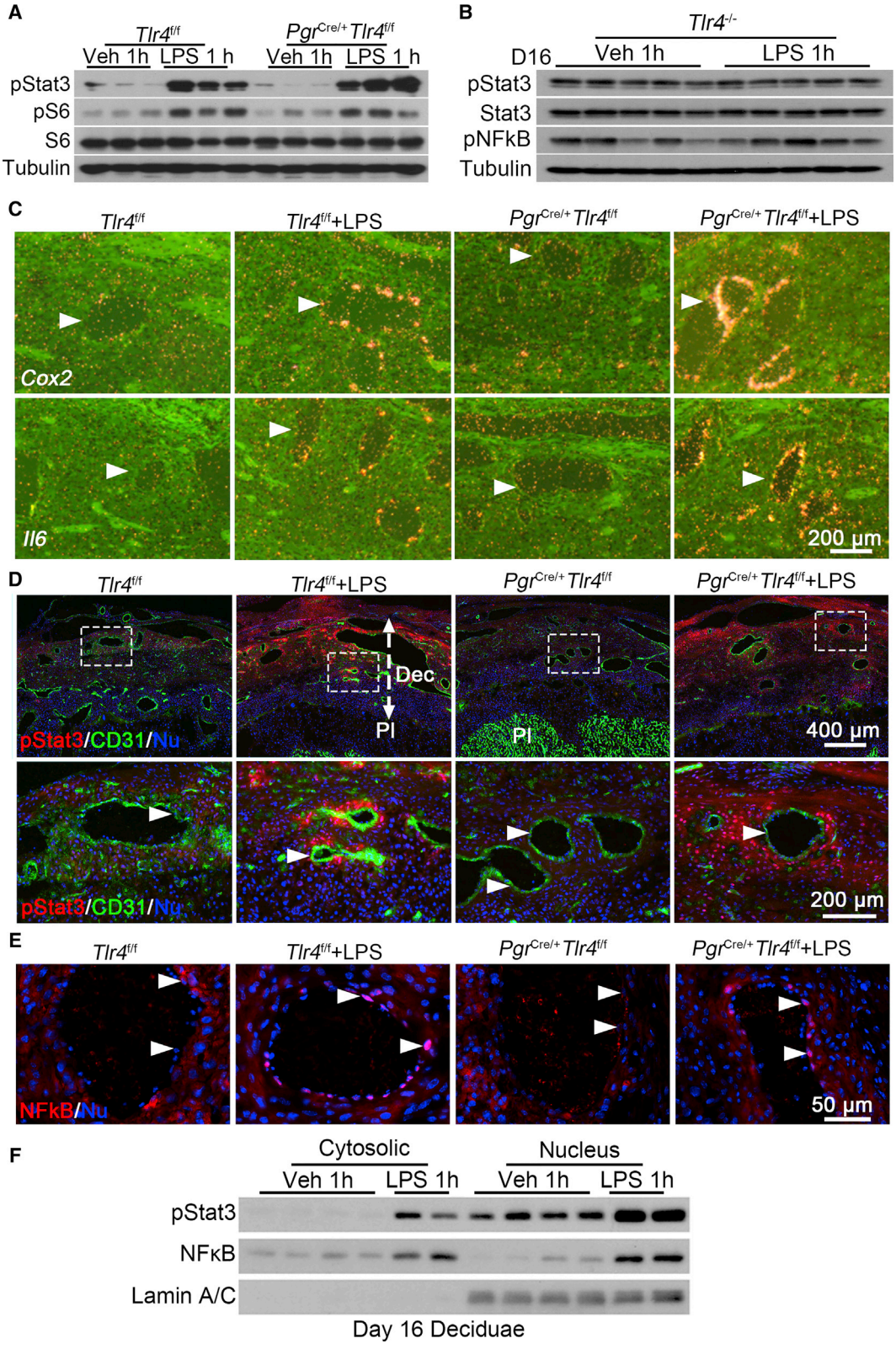

(legend on next page)

and decidual vascular endothelial cells than those in placental cells (Figure S1E) (Suryawanshi et al., 2018). Higher expression of TLR4 in the human endometrium compared with other members is also seen in apparently normal patients in the TCGA (The Cancer Genome Atlas) database (Figure S1F). Taken together, these results suggest that TLR4 in human decidual cells may respond to inflammation/infection similar to that noted in mice.

Role of TLR4 in Decidual Stromal Cells versus Decidual Endothelial Cells

These results led us to explore the site of TLR4-mediated function in the pregnant mouse uterus. Our previous study showed that genetically predisposed mice are extremely sensitive to ultra-pure TLR4-specific LPS to induce PTB (Cha et al., 2013; Deng et al., 2016). However, the homeostatic balance between inflammatory and anti-inflammatory responses remains unknown. Because progesterone receptors are expressed in all major uterine cell types, we generated conditional *Tlr4* mutant mice using *Pgr*-Cre driver ($Pgr^{Cre/+}Tlr4^{f/f}$) to investigate the physiological significance of TLR4 in the decidua (Figures 1C and S2A-S2C). Increased incidence of embryo resorption is observed in some mothers on day 16 but not apparent on day 8, along with decreased live litter sizes, indicates an important role of TLR4 during pregnancy (Figures 1D–1F). We speculated that mice with decidual deletion of *Tlr4* should be resistant to LPS, similar to that observed in *Tlr4* systematic knockout mice ($Tlr4^{-/-}$) (Wahid et al., 2015). Unexpectedly, these $Pgr^{Cre/+}Tlr4^{f/f}$ mice show exquisite sensitivity to PTB even upon an exposure to a low dose of LPS; LPS at 2.5 μg/mouse widely induces PTB (82%) with 92% dead pups. This low dose does not elicit adverse effects in $Tlr4^{f/f}$ pregnant mice (Figures 1G and S2D). One may argue that increased sensitivity of $Pgr^{Cre/+}Tlr4^{f/f}$ mice is due to compromised TLR4 activity in resident leucocytes. However, co-staining of CD45, dolichos biflorus agglutinin (DBA)-lectin (natural killer [NK] cells), F4/80, Ly6G, and CD4 with PR in day 16 deciduae shows no overlap, excluding the possibility of deletion of TLR4 by the *Pgr*-Cre driver in decidual leucocyte populations (Figure S2E). Non-uterine tissues, such as spleen and liver, do not show specific PR staining (Figure S3). Using T cell-specific deletion of PR and glucocorticoid receptor (GR), it was shown that P_4-induced T cell death is mediated by GR but not PR (Hirweger et al., 2019). In a recent study, single-cell analysis of human decidual cells in the first trimester shows that PR expression is very low to undetectable in NK cells, dendritic cells (DCs), monocytes, macrophages, and T cells as opposed to a significant presence of GR expression in these cell types. PR is primarily expressed in stromal cells (Vento-Tormo et al., 2018).

IL-6 is considered important for both LPS-induced PTB and normal delivery because the loss of *Il6* shows delayed parturition and resists LPS-triggered PTB (Robertson et al., 2010). To investigate responses of LPS over time, $Tlr4^{f/f}$ mice were treated with LPS (2.5 μg) for 1, 3, and 6 hours. Both *Il6* and *Il10* were rapidly induced at 1 hour followed by their gradual downregulation. *Cox2* was also induced at 1 hour with further increases at 3 and 6 hours (Figures S4A–S4C). Co-staining of CD31 and Cox2 presents evidence that Cox2 is induced in the endothelial cells (Figure S4D). The finding of rapid induction of *Il6* and *Il10* in day 16 decidua by LPS led us to analyze the expression of these cytokines in $Tlr4^{f/f}$ and $Pgr^{Cre/+}Tlr4^{f/f}$ mice. Surprisingly, the expressions of *Il6* and *Il10* are significantly induced in the decidua by LPS in both $Tlr4^{f/f}$ and $Pgr^{Cre/+}Tlr4^{f/f}$ mice with no induction of these cytokines in *Tlr4* systematic knockout mice (Figures 1H and 1I).

Cross-Talk between Endothelial Cells and Perivascular Stromal Cells

To further evaluate LPS-induced signaling pathways, nuclear factor kappa B (NF-κB) and pStat3, critical mediators of inflammatory and anti-inflammatory responses, respectively, in the context of cell types and experimental conditions, were investigated after LPS injection. Western blotting analysis shows that induction of pStat3 by LPS in $Tlr4^{f/f}$ and $Pgr^{Cre/+}Tlr4^{f/f}$ mice is comparable with no pStat3 induction in TLR4 systemic knockout mice (Figures 2A and 2B). Our ISH results also show that *Il6* and *Cox2* are induced in endothelial cells of $Pgr^{Cre/+}Tlr4^{f/f}$ deciduae after LPS treatment, similar to that of $Tlr4^{f/f}$ mice on day 16 (Figure 2C). Immunofluorescence (IF) as well as results of isolated cytoplasm and nuclei reveal perivascular localization of pStat3 and nuclear translocation of NF-κB in endothelial cells in $Pgr^{Cre/+}Tlr4^{f/f}$ deciduae, which are similar to $Tlr4^{f/f}$ mice after LPS exposure (Figures 2D–2F). The localization of pStat3 in the decidual cells and CD31 in endothelial cells (Figures 2D, S4E, and S4F) indicates a cross-talk between perivascular stromal cells and endothelial cells.

Endothelial-Specific Deletion of *Tlr4* Protects against LPS-Induced PTB

Undiminished TLR4 response in $Pgr^{Cre/+}Tlr4^{f/f}$ mice suggested another site of activation of TLR4 mediates its response to

Figure 2. Interactions between Endothelial and Perivascular Stromal Cells in the Decidual Bed of $Pgr^{Cre/+}Tlr4^{f/f}$ Mice

(A) Western blotting of pStat3 and pS6 levels in day 16 uteri of $Tlr4^{f/f}$ and $Pgr^{Cre/+}Tlr4^{f/f}$ dams exposed to LPS (2.5 μg/mouse), n = 3.

(B) Western blotting results of pStat3, Stat3, and pNFκB levels in day 16 deciduae after LPS treatment for 1 hour in $Tlr4^{-/-}$ mice, n = 5.

(C) *In situ* hybridization for *Cox2* and *Il6* mRNAs in $Tlr4^{f/f}$ and $Pgr^{Cre/+}Tlr4^{f/f}$ mice after exposure to LPS for 1 hour. Arrowheads indicated endothelial cells. Scale bar, 200 μm.

(D) Immunofluorescence staining of pStat3 (red) and CD31 (green) in $Tlr4^{f/f}$ and $Pgr^{Cre/+}Tlr4^{f/f}$ mice after exposure to LPS for 1 hour. Scale bar of upper panels, 400 μm. Bottom panels show images at higher magnification of those within the demarcated rectangles in the upper panels. Dec, decidua; Pl, placenta. Arrowheads indicate endothelial cells. Scale bar, 200 μm.

(E) Immunostaining showing nuclear NF-κB (red) in $Tlr4^{f/f}$ and $Pgr^{Cre/+}Tlr4^{f/f}$ mice after exposure to LPS for 1 hour. Arrowheads indicate endothelial cells. Scale bar, 50 μm.

(F) Western blotting for pStat3 and NF-κB in cytosolic and nuclear fractions of day 16 deciduae after 1 h of vehicle or LPS treatment in $Tlr4^{f/f}$ females. Lamin AC was used as nuclear internal control.

See also Figures S2, S3, and S4.

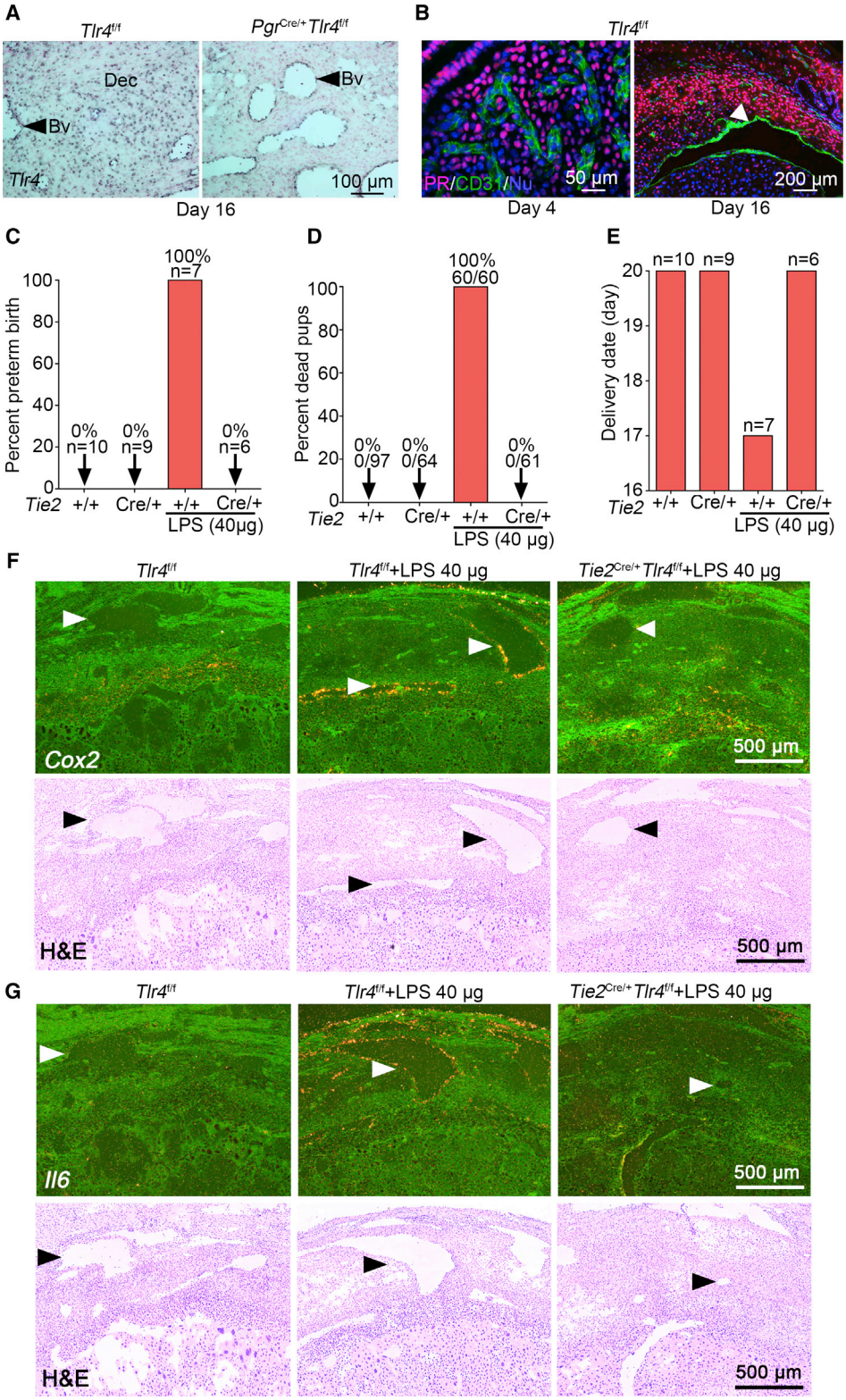

Figure 3. Endothelial-Specific *Tlr4* Deletion with a *Tie2-Cre* Driver Protects against LPS-Induced Preterm Birth

(A) DIG-*in situ* hybridization for *Tlr4* in decidual endothelia of $Tlr4^{f/f}$ and $Pgr^{Cre/+}Tlr4^{f/f}$ mice on day 16 of pregnancy. Blue color indicates the *Tlr4* signal. Dec, decidua. Arrow heads indicate blood vessels (Bv). Scale bar, 100 μm.

(legend continued on next page)

LPS. Induction of *Il6* and *Cox2* in endothelial cells led us to speculate that decidual endothelial TLR4 might contribute to this disparity. To explore if endothelial TLR4 sufficiently responds to LPS exposure, we first confirmed the expression of *Tlr4* in both $Tlr4^{f/f}$ and $Pgr^{Cre/+}Tlr4^{f/f}$ mice. The persistent expression of *Tlr4* in $Pgr^{Cre/+}Tlr4^{f/f}$ endothelial cells suggests that endothelial TLR4 is an effective sensor to propagate LPS signaling to induce PTB because *Pgr-Cre* is incapable of deleting endothelial *Tlr4* (Figure 3A). Indeed, co-staining of PR and CD31 clearly shows that endothelial cells in days 4 and 16 uterus are PR negative during pregnancy (Figure 3B). We investigated the significance of endothelial TLR4 by using a *Tie2-Cre* driver to circumvent the limitation of the *Pgr-Cre* driver. The results from $Tie2^{Cre/+}Rosa26^{Tomato}$ reporter mice show that *Tie2-Cre* is primarily expressed in blood vessel endothelia in the decidua (Figure S4G). We also observed that *Tie2-Cre* does not show any recombination in immune cells, indicating *Tie2* expression is specific to endothelial cells, which was verified by the absence of tomato reporter in the stromal compartment (Figure S4G). The deletion efficiency of *Tlr4* was confirmed by qPCR and digoxin (DIG)-ISH (Figures S4H and S4I). $Tie2^{Cre/+}Tlr4^{f/f}$ mice exposed to LPS show normal litter size and parturition without any apparent adverse effects on viability and growth rate of pups or apparent distress of the mother upon delivery (Figures 3C–3E and S4J). In contrast to $Pgr^{Cre/+}Tlr4^{f/f}$ mice, LPS at a low dose (2.5 μg/mouse) does not provoke harmful effects in $Tlr4^{f/f}$ or $Tie2^{Cre/+}Tlr4^{f/f}$ mice. $Tie2^{Cre/+}Tlr4^{f/f}$ mice were then challenged with a higher dose of LPS (40 μg/mouse). Although 100% of $Tlr4^{f/f}$ mice show PTB at this high dose, no observable deleterious effects were noted in $Tie2^{Cre/+}Tlr4^{f/f}$ mice. They show normal litter sizes and parturition timing (Figures 3C–3E). The total abrogation of LPS-induced PTB in $Tie2^{Cre/+}Tlr4^{f/f}$ mice suggests that endothelial TLR4 activation is indispensable for LPS-triggered signal transduction in the decidua.

To better understand the underlying cause of LPS resistance in $Tie2^{Cre/+}Tlr4^{f/f}$ mice, we examined the expression of inflammation-associated cytokines in $Tlr4^{f/f}$ and $Tie2^{Cre/+}Tlr4^{f/f}$ mice in the absence or presence of LPS. The expression of *Cox2* and *Il6* is primarily induced in endothelial cells of $Tlr4^{f/f}$ mice by LPS but not in $Tie2^{Cre/+}Tlr4^{f/f}$ mice (Figures 3F and 3G). Our fluorescence ISH (RNA-FISH) coupled with *Il6* DIG probe is consistent with radioactive ISH results (Figure S4K). qPCR results show that both *Il6* and *Il10* are induced at low and high doses (2.5 or 40 μg/mouse) of LPS in $Tlr4^{f/f}$ mice, whereas these inductions are not seen in $Tie2^{Cre/+}Tlr4^{f/f}$ mice (Figures 4A and 4B). We also observed higher induction of *Il6* in $Tlr4^{f/f}$ mice in the presence of a higher dose of LPS (Figure 4A). The decreased ratio of expression *Il10*/*Il6* in $Tlr4^{f/f}$ mice at a high dose of LPS further supports that the balance between pro-inflammation and anti-inflammation is disturbed under higher LPS dose in floxed mice (Figure 4C). This imbalance of IL-10 and IL-6 is likely to account for PTB at a higher dose of LPS.

IL-6 Can Activate Stat3 and *Il10* Expression in Decidual Cells in Culture

Activation of Stat3 (pStat3) is seen in $Tlr4^{f/f}$ deciduae after LPS exposure, but this activation is absent in $Tie2^{Cre/+}Tlr4^{f/f}$ mice after exposure to LPS (Figures 4D and 4E). To examine if IL-6 can directly activate Stat3, isolated stromal cells from pregnant day 4 uterus were cultured to decidualized cells by estrogen and P_4 (Deng et al., 2016), followed by exposure to IL-6. We found significant nuclear pStat3 enrichment and elevated pStat3 levels along with higher *Il10* mRNA levels (Figures 4F–4H). IL-6 mediates its function by engaging IL-6 receptor (Il6r) and Gp130 to trigger Stat3 phosphorylation (Johnson et al., 2018). ISH results show expression of *Il6r* and *Gp130* in the decidua (Figure S5A). qPCR results show that their expression levels are comparable in both genotypes with or without LPS exposure (Figure S5E).

Furthermore, cytoplasmic NF-κB fails to translocate to endothelial cell nuclei after LPS treatment in $Tie2^{Cre/+}Tlr4^{f/f}$ mice (Figure 5A). CD14 is a co-receptor of TLR4 for LPS binding and cellular uptake; its expression is dependent on NF-κB signaling (Zanoni et al., 2011). Our results show that CD14 is primarily induced by LPS in endothelial cells in $Tlr4^{f/f}$ mice but not in $Tie2^{Cre/+}Tlr4^{f/f}$ mice, suggesting that NF-κB activation in the endothelium is abrogated in $Tie2^{Cre/+}Tlr4^{f/f}$ mice (Figures 5B and 5C).

Resident Decidual Immune Cells Are Not a Target of LPS

Because immune cells are considered a major source of cytokines, we examined the distribution of immune cells in deciduae after exposure to LPS. An abundant population of uterine NK (uNK) cells were noted in deciduae of both $Tlr4^{f/f}$ and $Tie2^{Cre/+}Tlr4^{f/f}$ mice, but their distribution patterns were comparable after LPS challenge in the presence or absence of endothelial TLR4 (Figure S5B). As Stat3 is important for the production of cytokines in NK cells (Saraiva and O'Garra, 2010), we explored if pStat3 is activated in uNK cells after LPS treatment. Co-staining shows that pStat3 and uNK cells are rarely co-localized in the presence of LPS (Figure S5C). The unaltered expression of GzmA and GzmC, major markers of NK cells, is consistent with the finding of unaltered distribution of uNKs (Figures S5D and S5E).

The number of macrophages is scanty in the decidua and restricted in the myometrium as previously reported (Nancy et al., 2012; Tachi and Tachi, 1986). Macrophage population

(B) PR (progesterone receptor)-positive cells are absent in the endothelium in days 4 (left) and 16 (right) uteri. Arrow head indicates blood vessel. Scale bars for the left and right panels represent 50 μm and 200 μm, respectively.
(C and D) The ratio of preterm birth (C) and dead pups (D) compared to total number of pups in $Tlr4^{f/f}$ and $Tie2^{Cre/+}Tlr4^{f/f}$ mice with or without a high dose of LPS (40 μg/mouse). n, number of dams examined.
(E) Parturition timing in $Tlr4^{f/f}$ and $Tie2^{Cre/+}Tlr4^{f/f}$ mice with or without LPS. n, number of dams examined.
(F) Dark-field and bright-field images of *in situ* hybridization for *Cox2* in $Tlr4^{f/f}$ and $Tie2^{Cre/+}Tlr4^{f/f}$ deciduae after 1 h of LPS exposure (40 μg/mouse). Arrow heads indicate blood vessels. Scale bar, 500 μm.
(G) Dark-field and bright-field images of *in situ* hybridization for *Il6* in $Tlr4^{f/f}$ and $Tie2^{Cre/+}Tlr4^{f/f}$ deciduae after 1 h of LPS exposure (40 μg/mouse). Arrow heads indicate blood vessels. Scale bar, 500 μm.
See also Figure S4.

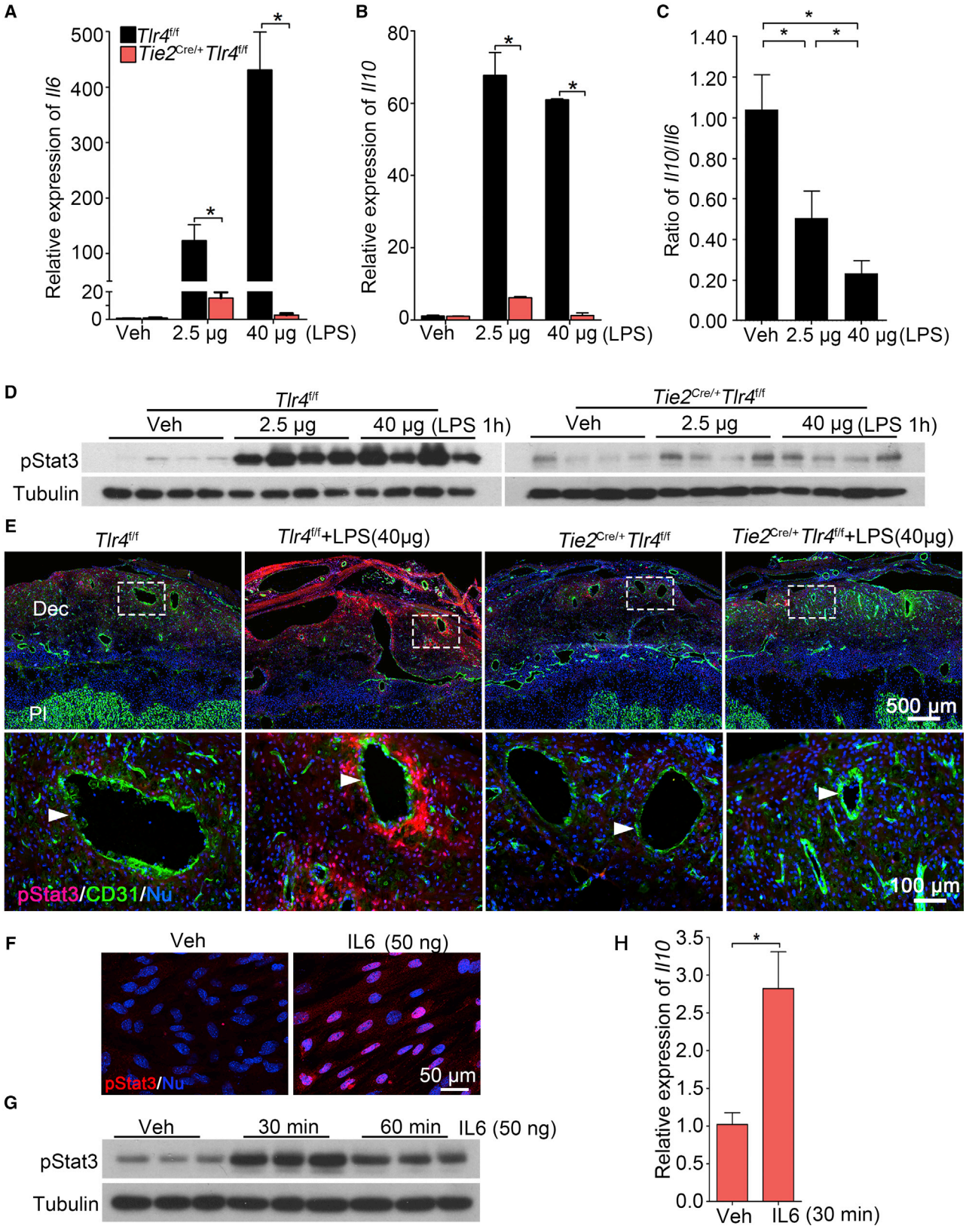

(legend on next page)

remains unchanged before and after LPS challenge for 1 and 6 hours (Figures S6 and S7) and that neutrophil distribution was rare in uterine decidua even after LPS exposure; only a few are seen adhered to the endothelium (Figures S6 and S7). The staining of CD45, a common marker of leukocytes, also did not show obvious changes in distribution (Figures S6 and S7), suggesting that endothelial TLR4 is minimally or not engaged with immune cells to produce cytokines in the decidua to provoke PTB. Similar to $Pgr^{Cre/+}Tlr4^{f/f}$ mice, the immune cells do not exhibit PR expression in $Tie2^{Cre/+}Tlr4^{f}$ mice (Figures S6 and S7).

The Ovary Is Not a Target of PTB When LPS Is Given on Day 16

There are reports that LPS targets the ovary and induces PTB by reducing P_4 levels (Aisemberg et al., 2013; Cha et al., 2013). Our results show that *Tlr4* expression is quite low in the ovary (Figure 1B), and evidence suggests that decidual health, as evident from the expression of *PlpJ* and *Prlr*, is critical for the functional lifespan of the corpus luteum (Cha et al., 2013). To circumvent the effects of LPS-induced ovarian steroid hormonal changes, day 16 pregnant females were ovariectomized and injected with a combination of hormones, which maintains pregnancy with normal parturition timing. In contrast, an LPS (40 μg) injection on day 16 along with similar hormones injections induces PTB within 48 hours with stillbirths (Figures 6A and 6B). Considering the high abundance of TLR4 expression in the decidua with rapid response to LPS, these results strongly support that the decidua is a direct target of LPS and by inference other bacterial infections. Downregulation of *Prlr* by LPS in $Tlr4^{f/f}$ mice but not in $Tie2^{Cre/+}Tlr4^{f/f}$ mice further supports that LPS dampens decidual health through endothelial TLR4 (Figures 6C and 6D).

IL-10 Confers Protection against PTB in Response to Inflammation

IL-10 is an anti-inflammatory cytokine and safeguards against infection or inflammation, and Stat3 is considered a major regulator of IL-10 expression (Saraiva and O'Garra, 2010). The mining of the published chromatin immunoprecipitation sequencing (ChIP-seq) database suggests a potential Stat3 binding site at the downstream region of *Il10* gene and histone modification at the promoter region (Figures 6E and 6F). We verified the binding by ChIP-qPCR by using both pStat3 and Stat3 antibodies as well as H3K4me3 antibody in LPS-treated decidua (Figures 6G and 6H); samples from untreated uteri were below the detection levels. Our results suggest that IL-10 is transcriptionally and epigenetically regulated by LPS.

We next asked if neutralization of IL-10 enhances PTB incidence. IL-10 knockout mice are extremely sensitive to external infection and show inflammatory bowel disease syndrome (Kühn et al., 1993). Therefore, we adopted a different approach to neutralize endogenous IL-10. A neutralizing antibody to IL-10 (500 μg/mouse) was injected into both wild-type (WT) ($p53^{f/f}$) and PTB predisposed mice ($Pgr^{Cre/+}p53^{f/f}$) 30 min before and after an LPS injection on day 16 to monitor parturition timing (Clemente-Casares et al., 2016). We found increased incidence of PTB in both genotypes even at a dose as low as 1 μg/mouse LPS with increased incidence of PTB in predisposed mice (Figures 7A and 7B). Normally, administration of 2.5 μg LPS does not lead to any adverse pregnancy effects in $p53^{f/f}$ (WT) mice, but administration of an IL-10 neutralizing antibody substantially increases the sensitivity of these mice to LPS. To better understand the underlying mechanism of increased PTB rate upon IL-10 inhibition, decidualized stromal cells were treated with an anti-IL-10 antibody. Increased phosphorylated nuclear factor NF-kappa-B (pNFκB) levels indicate heightened inflammation after administration of IL-10 neutralizing antibody (Figure 7C). pS6 levels are also substantially elevated by the IL-10 antibody (Figure 7C), mimicking some aspects of LPS-treated deciduae (Figure 2A). Notably, higher levels of *Il6*, *Tnf*, and *Il1β* after IL-10 neutralization also suggest the anti-inflammatory role of IL-10 in decidualized stromal cells (Figures 7D–7F). Our previous results suggest that increased mTORC1 signaling is an important determinant of PTB. Thus, increased pS6 levels by LPS and anti-IL-10 indicates that the function of IL-10 in parturition at least partially influences the mTORC1 signaling pathway, which is supported by a recent study (Ip et al., 2017).

DISCUSSION

Our observation of abundant expression of TLR4 in the decidua suggests that the signal transduced by this member of the TLR family plays a functional role during normal pregnancy. In this respect, the findings of highest levels of *Tlr4* mRNA among the other family members in the decidua support TLR4 function in pregnancy outcomes. In contrast, surprisingly low levels of *Tlr4* expression in the placenta suggest that the decidua plays a major role in modulating systemic infection or inflammation during pregnancy, although placental roles in regulating inflammatory and anti-inflammatory responses under local microbial infection cannot be ruled out. We have provided evidence that endothelial TLR4 in coordination with perivascular stromal cells in the decidual bed calibrates the degree of inflammatory and

Figure 4. Endothelial TLR4 Is Critical for Sensing LPS-Induced Responses in Decidua

(A and B) Relative expression of *Il6* (A) and *Il10* (B) mRNAs in $Tlr4^{f/f}$ and $Tie2^{Cre/+}Tlr4^{f/f}$ mice after a low dose (2.5 μg/mouse) or high dose (40 μg/mouse) of LPS treatment for 1 hour. n = 4. *p < 0.05. Results are shown as mean ± SEM.

(C) Ratio of mRNA levels of *Il10* versus *Il6* in deciduae of $Tlr4^{f/f}$ mice under a low and high dose of LPS. n = 4. *p < 0.05. Results are shown as mean ± SEM.

(D) western blotting of protein levels for pStat3 in $Tlr4^{f/f}$ and $Tie2^{Cre/+}Tlr4^{f/f}$ mice after 1 h of a low or high dose of LPS treatment on day 16 of pregnancy, n = 4.

(E) Co-immunostaining of pStat3 (red) and CD31 (green) in LPS-treated deciduae of $Tlr4^{f/f}$ and $Tie2^{Cre/+}Tlr4^{f/f}$ mice. Scale bar of upper panels, 500 μm. Bottom panels show images of higher magnification of those within the demarcated rectangles (Scale bar, 100 μm). Arrowheads indicate endothelial cells. Dec, deciduae; Pl, placenta.

(F) pStat3 nuclear translocation by IL-6. Isolated stromal cells were treated with recombinant IL-6 (50 ng) for 30 min. Scale bar, 50 μm.

(G and H) pStat3 levels (G) and *Il10* mRNA levels (H) after recombinant interleukin 6 (rIL-6) challenge. Tubulin and *rpL7* were used as internal controls for western blotting and qPCR, respectively. n = 3. *p < 0.05. Results are shown as mean ± SEM.

See also Figures S5, S6, and S7.

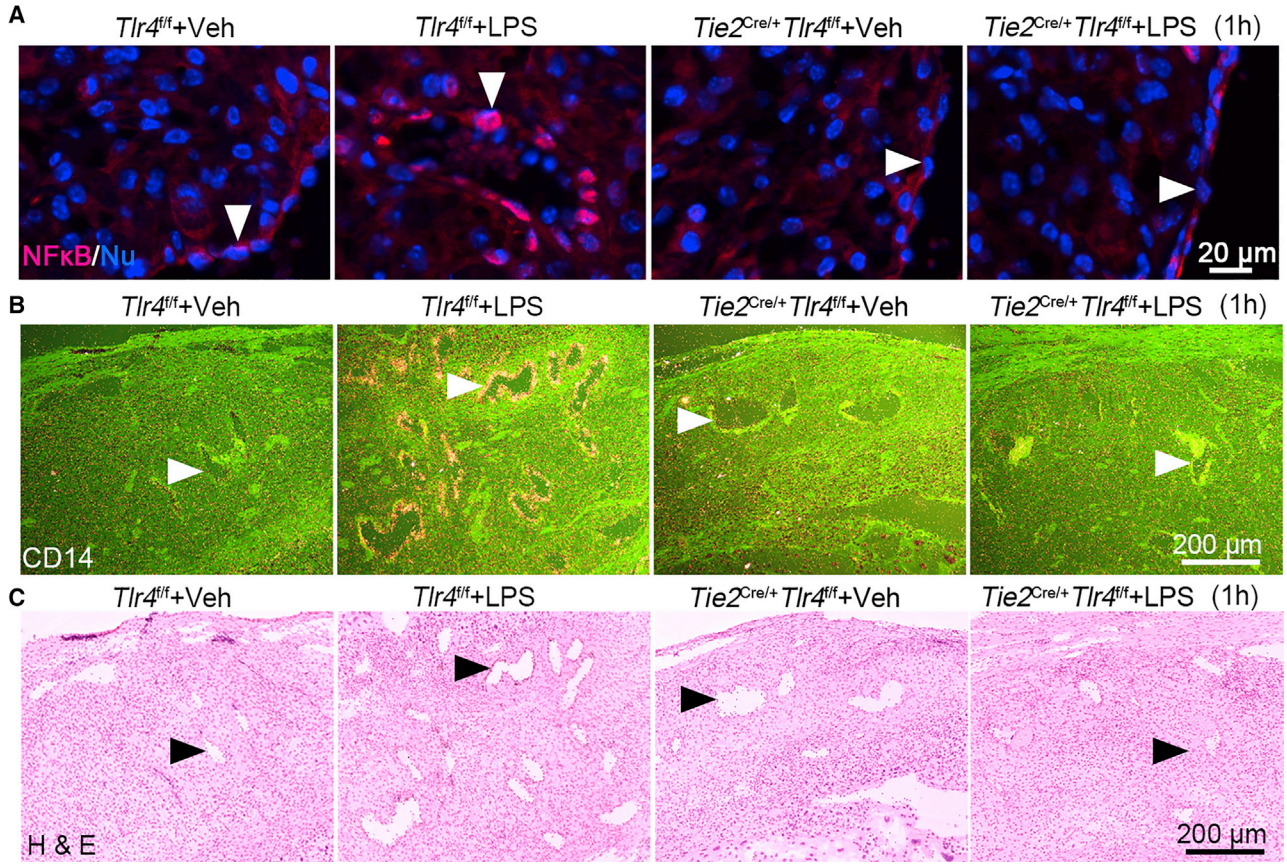

Figure 5. Endothelial NF-κB and CD14 Are Downregulated in *Tie2*$^{Cre/+}$*Tlr4*$^{f/f}$ Deciduae

(A) Immunostaining shows nuclear translocation of NF-κB (red) in *Tlr4*$^{f/f}$ and *Tie2*$^{Cre/+}$*Tlr4*$^{f/f}$ mice after exposure to LPS (40 μg/mouse) for 1 hour. Arrow heads indicate endothelial cells. Scale bar, 20 μm.

(B and C) LPS-induced expression of *Cd14* by radioactive *in situ* hybridization (B) in day 16 decidual endothelial cells in *Tlr4*$^{f/f}$ and *Tie2*$^{Cre/+}$*Tlr4*$^{f/f}$ mice. The lower panel (C) represents H&E-stained images. Arrow heads indicate endothelial cells. Scale bar, 200 μm.

anti-inflammatory responses to inflammation in pregnancy. The role of endothelial TLR4 has not been widely explored in other systems, although our results are consistent with only two published reports showing a protective role of endothelial TLR4 deletion in the intestine and brain (Tang et al., 2017; Yazji et al., 2013). Here, we show that endothelial TLR4 in the decidual bed is also a major target for inflammation-induced PTB, but the function of decidual TLR4 remains obscure. However, compromised pregnancy outcomes of *Pgr*$^{Cre/+}$*Tlr4*$^{f/f}$ mice in the absence of LPS and sensitivity of these mice to LPS driving PTB suggest that decidual TLR4 has a role in pregnancy, the function of which is not clearly understood at this time and is a subject of future investigation.

In this study, we provide evidence that the decidua functions as a rheostat to establish a homeostatic balance between inflammation and anti-inflammation following infection or inflammation in pregnancy, and this balance is crucial to pregnancy success. This study shows that the decidua is endowed with anti-inflammatory activity that can offset certain inflammatory responses. Under infection or inflammation, the dynamic balance is challenged, and PTB occurs if the degree of inflammation is excessive. Our results illustrate a rapid inflammatory response after LPS challenge in day 16 deciduae that gradually decreases to a basal level. The prompt release of inflammatory cytokines after LPS exposure often generates an inflammatory cytokine stress in genetically predisposed mice, such as *Pgr*$^{Cre/+}$*p53*$^{f/f}$ mice (Hirota et al., 2010) or *Pgr*$^{Cre/+}$*Tlr4*$^{f/f}$ mice. These mice experience PTB, even after a small dose of LPS challenge that is tolerable in normal pregnant mice.

The expression of IL-6 and Cox2 in decidual endothelial cells and induction of pStat3 in the nuclei of perivascular decidual cells following LPS stimulation perhaps initiate a cascade of signaling events. Myometrial contractions driven by increased prostaglandin $F_{2\alpha}$ ($PGF_{2\alpha}$) is considered important for delivery. However, previous and present results show that Cox2 expression is primarily expressed in the decidual stromal cells and endothelial cells, but not muscle cells, under normal and after LPS challenge. These results suggest that PGs originating in the decidua influence myometrial contractility (Hirota et al., 2010). Because IL-6 is known to activate Stat3 (Johnson et al., 2018; Yasukawa et al., 2003), it is assumed that IL-6 induces perivascular Stat3 phosphorylation, which is promptly followed

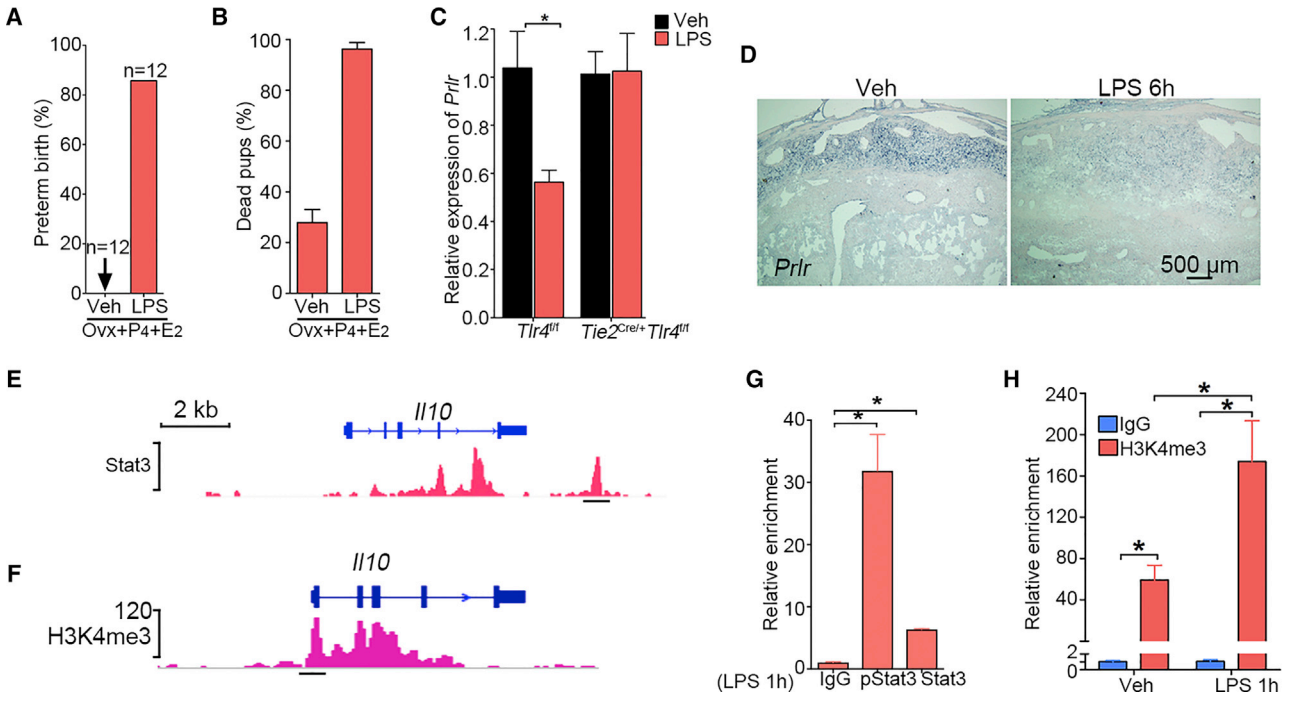

Figure 6. LPS Targets Deciduae, Not Ovaries, and Regulation of IL-10 by Stat3

(A) Incidence of PTB in pregnant mice ovariectomized on day 16 with or without exposure to LPS (40 μg/mouse) followed by P_4 injections (1 mg) on days 16 and 17 and 250 μg of P_4 on day 18 with an additional injection of estradiol-17β (100 ng) on day 19. All ovariectomized (Ovx) mice given P_4 and E_2 without LPS showed normal delivery, albeit 40% dead pups. In contrast, over 90% of LPS-treated mice delivered dead pups before day 19 with 100% dead pups. Ovx, ovariectomy. n, number of mice examined in each group.

(B) Rate of dead pups in mice with or without LPS injection after ovariectomy followed by P_4 and E_2 injection. n = 12.

(C) Relative expression of *Prlr* mRNA in $Tlr4^{f/f}$ and $Tie2^{Cre/+}Tlr4^{f/f}$ mice after exposure to LPS (40 μg/mouse) for 1 hour. n = 4, *p < 0.05. Results are shown as mean ± SEM.

(D) DIG-*in situ* hybridization for *Prlr* in $Tlr4^{f/f}$ mice after 6 h of LPS (40 μg/mouse) treatment. Scale bar, 500 μm.

(E and G) Graphic representation of predicted Stat3 binding site on the *Il10* gene (E) and ChIP-qPCR confirmation of binding by both pStat3 and Stat3 antibodies in deciduae after LPS injection for 1 h (G). n = 3, *p < 0.05. Data are represented as mean ± SEM.

(F and H) Graphic representation of H3K4me3 enrichment at the *Il10* promoter region (F) with ChIP-qPCR confirmation in deciduae after LPS injection for 1 h (H). n = 3, *p < 0.05. Data are represented as mean ± SEM.

by anti-inflammatory responses as a protective measure, as seen in WT mice in response to mild inflammation (low LPS doses) to preserve pregnancy. PTB ensues if the initial inflammatory response is overwhelming and overcomes physiologic anti-inflammatory responses, as seen in PTB-predisposed mice. Enhanced expression of pro-inflammatory mediators with dysfunctional anti-inflammatory pathways in Stat3-deleted macrophages and neutrophils suggests anti-inflammatory effects of Stat3 (Takeda et al., 1999). We suspect that pStat3 in decidual cells also confers protection against inflammation by regulating IL-10 expression, which is supported by studies in other systems (Saraiva and O'Garra, 2010). IL-10 is one of the earliest identified anti-inflammatory cytokines upregulated after LPS injection (Manzanillo et al., 2015). Our findings of increased decidual levels of IL-10 by LPS suggest that this cytokine plays a critical role in maintaining a homeostatic balance between the pro- and anti-inflammatory responses to resist PTB within a certain limit of infection or predisposition.

It is possible that resident immune cells in the decidua have a role in responding to LPS exposure in pregnancy. Although it cannot be completely excluded, our results show comparable distribution of CD45-positive cells in $Tlr4^{f/f}$ and $Tie2^{Cre/+}Tlr4^{f/f}$ deciduae after LPS treatment. These results suggest that immune cells do not play a major role in generating cytokines at the early stage of LPS challenge in the decidua. This is consistent with the observation that T cells and macrophages are predominantly confined to the myometrium in normal pregnancy (Nancy et al., 2012; Tachi and Tachi, 1986). Notably, deciduae on day 16 shows abundant NK (uNK) cells, which are thought to participate in vessel remodeling and nourishing the developing embryo (Fu et al., 2017). However, the distribution of uNK cells remains unaltered in the decidua after LPS treatment. In this context, our results suggest that decidual endothelial cells are endowed with a function that was previously attributed to immune cells.

It is possible that increases in inflammatory circulating cytokines originating from other organs contribute to PTB after LPS challenge. Whether circulating cytokines can directly target endothelial cells and then stromal cell gene expression is not known. It is more reasonable that local production of these cytokines by endothelial TLR4 in response to LPS or gram-negative

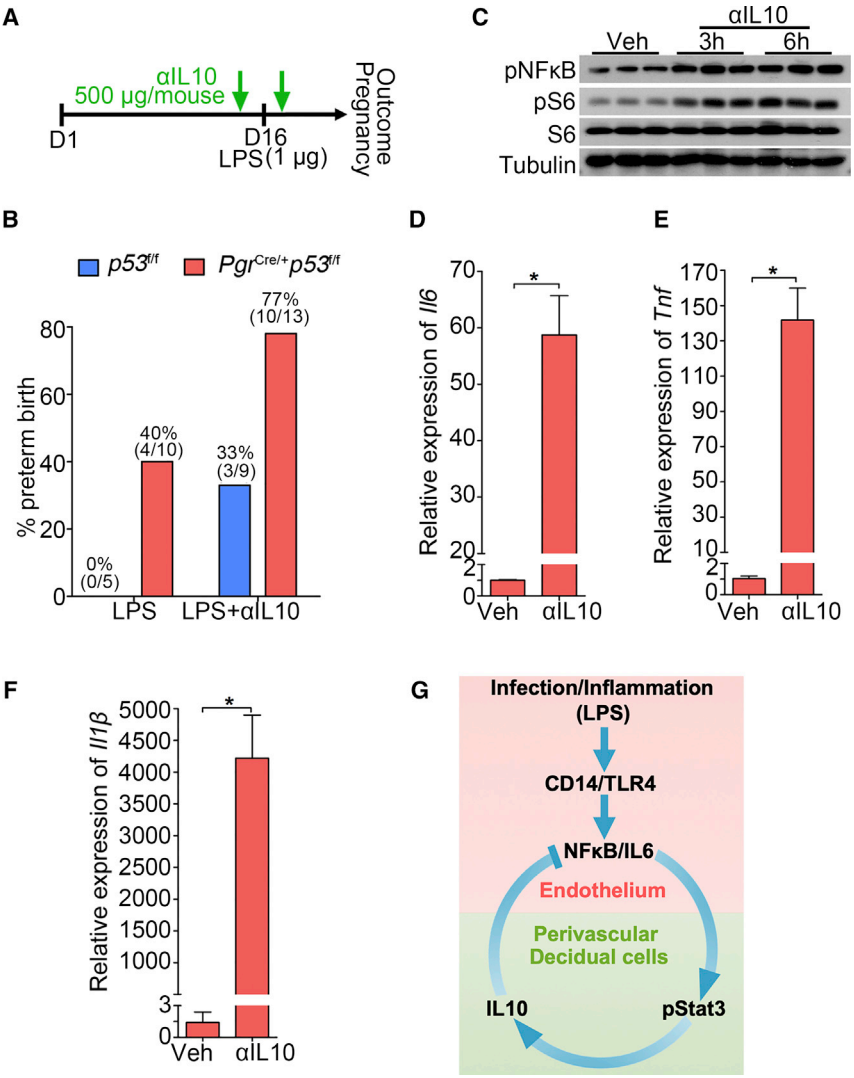

Figure 7. The Role of IL-10 in PTB Prevention

(A) A scheme of treatment schedule of IL-10 neutralizing antibody (αIL-10).

(B) Preterm birth rate of $p53^{f/f}$ and $Pgr^{Cre/+}p53^{f/f}$ mice after IL-10 neutralizing antibody (αIL-10) injection in the presence of a ultra-low dose of LPS exposure (1 μg/mouse). The number in parentheses indicates the incidence of PTB in total number of mice analyzed.

(C) Western blot results for pNFκB and pS6 levels in decidualized stromal cells after IL-10 neutralizing antibody treatment for 3 and 6 hours.

(D–F) *Il6* (D), *Il1b* (E), and *Tnf* (F) mRNA levels by IL-10 neutralizing antibody treatment. n = 3, *p < 0.05. Data are represented as mean ± SEM (n = 3).

(G) A representative scheme of a physiological role of endothelial TLR4 in LPS-induced inflammation. After binding with LPS, endothelial TLR4 directs NFκB nuclear translocation to stimulate endothelial IL-6 expression in endothelial cells. Locally generated IL-6 stimulates Stat3 phosphorylation in perivascular decidual cells for IL-10 expression. Activation of endothelial TLR4 by LPS, which counters endogenous IL-10 production, results in preterm birth. CD14 is a co-receptor for TLR4 and highly induced in endothelial cells after LPS stimulation.

bacteria would induce gene expression in a paracrine manner in perivascular stromal cells in the decidua. A comprehensive understanding to address this issue would necessitate generation of endothelial-specific Cre drivers for each organ, but this is a daunting task with the current state of our knowledge. Nonetheless, a critical role of endothelial TLR4 to mount an inflammatory insult to pregnancy after an injection of LPS is profound. TLR4 expression and its functions in resident immune cells in the decidua and uterus in PTB are not clearly understood at this time. Under our experimental conditions, Tie2 and PR are not expressed in these immune cells. Furthermore, $Tie2^{Cre/+}Tlr4^{f/f}$ mice fail to evoke PTB with intact TLR4 in resident immune cells upon exposure to LPS even at a higher dose (40 μg/mouse). These results suggest that endothelial cell TLR4 is a primary inducer of PTB after LPS challenge.

Our previous studies have shown that decreased 5′-AMP-activated protein kinase (AMPK) signaling with heightened mTORC1 activity contributes to premature decidual aging, leading to increased predisposition to infection or inflammation and PTB (Cha et al., 2013; Deng et al., 2016; Hirota et al., 2011; Hirota et al., 2010). Therefore, restraining adverse effects of mTORC1 signaling by IL-10 could be a mechanism by which this anti-inflammatory cytokine protects pregnancy from inflammatory insults (Ip et al., 2017).

IL-10 expression is regulated by many pathways and transcription factors (Saraiva and O'Garra, 2010). The spatiotemporal relationship of Stat3 phosphorylation and IL-10 induction after LPS stimulation in deciduae strongly suggest a connection between them. Stat3 has been shown to promote both pro-inflammatory and anti-inflammatory effects through fine tuning of the expression of cytokines, such as IL-12 and IL-23 (Kortylewski et al., 2009), and a similar relationship between IL-10 and IL-6 is envisioned in the decidua, in which the ratio is likely to shift the balance toward or against a pro-inflammatory response in pregnancy. Our results of the ratio of *Il10/Il6* mRNAs toward pro-inflammation under high doses of LPS leading to PTB corroborate this conjecture.

The observation that TLR4-dependent nuclear translocation of NFκB in endothelial cells and Stat3 activation in the perivascular decidual stromal cells with induction of cytokines by LPS suggests that one function of the decidua is to counter infection or inflammation during pregnancy within a certain limit but fails to do so in genetically predisposed mothers to PTB. The function of TLR4 in humans is not clearly understood. One study suggests that TLR4 is one of the master regulators for human delivery through regulation of a cohort of gene expression (Lui et al., 2018).

Taken together, this work reveals a potential mechanism of anti-inflammatory activity of IL-10 regulated by endothelial TLR4 in deciduae (Figure 7G). We provide evidence of transcriptional regulation of IL-10 by Stat3 in the decidua. Considering that a similar signature of IL-10 expression and regulation operates in human deciduae, our findings may contribute to potential strategies to combat PTB. In conclusion, our present results put forward a concept that decidual endothelial cells are critical for mounting inflammation resulting from infection with subsequent activation of anti-inflammation machinery in late pregnancy.

STAR★METHODS

Detailed methods are provided in the online version of this paper and include the following:

- KEY RESOURCES TABLE
- CONTACT FOR REAGENT AND RESOURCE SHARING
- EXPERIMENTAL MODELS AND SUBJECT DETAILS
  - Animal care and housing
  - Cell cultures and treatments
- METHOD DETAILS
  - Analysis of pregnancy outcomes
  - Immunofluorescence (IF)
  - RNA Isolation and qPCR
  - Immunoblotting
  - Isolations of nuclei and cytoplasm
  - *In situ* hybridization
  - RNA-FISH
  - ChIP-PCR Assays
  - Identification of whole-genome binding sites of Stat3 and H3K4me3
  - Expression status of Tlrs identified by RNA-Seq analysis
- QUANTIFICATION AND STATISTICAL ANALYSIS
- DATA AND SOFTWARE AVAILABILITY

SUPPLEMENTAL INFORMATION

Supplemental Information can be found online at https://doi.org/10.1016/j.celrep.2019.04.049.

ACKNOWLEDGMENTS

Our sincere thanks to Katie Gerhardt for her efficient editing of the manuscript. We also thank Chris Karp and his group for proving the *Tlr4* floxed and systemic *Tlr4* mutant mice and Richard Lang for Tie2-Cre mice. This work was supported in part by NIH grants (R01HD068524, DA006668, and P01CA77839 to S.K.D.) and a center grant from the March of Dimes (22-FY17-889).

AUTHOR CONTRIBUTIONS

W.D., J.Y., J.C., X.S., and A.B. performed experiments. W.D. and S.K.D. designed experiments. H.Y. and Y.H. provided valuable reagents and tools. W.D., J.C., X.S., and S.K.D. analyzed data. W.D., J.C., Y.H., and S.K.D. wrote the manuscript.

DECLARATION OF INTERESTS

The authors declare no competing interests.

Received: December 4, 2018
Revised: March 18, 2019
Accepted: April 10, 2019
Published: May 7, 2019

REFERENCES

Aisemberg, J., Vercelli, C.A., Bariani, M.V., Billi, S.C., Wolfson, M.L., and Franchi, A.M. (2013). Progesterone is essential for protecting against LPS-induced pregnancy loss. LIF as a potential mediator of the anti-inflammatory effect of progesterone. PLoS One *8*, e56161.

Altmäe, S., Koel, M., Võsa, U., Adler, P., Suhorutšenko, M., Laisk-Podar, T., Kukushkina, V., Saare, M., Velthut-Meikas, A., Krjutškov, K., et al. (2017). Meta-signature of human endometrial receptivity: a meta-analysis and validation study of transcriptomic biomarkers. Sci. Rep. *7*, 10077.

Cha, J., Bartos, A., Egashira, M., Haraguchi, H., Saito-Fujita, T., Leishman, E., Bradshaw, H., Dey, S.K., and Hirota, Y. (2013). Combinatory approaches prevent preterm birth profoundly exacerbated by gene-environment interactions. J. Clin. Invest. *123*, 4063–4075.

Choukrallah, M.A., Song, S., Rolink, A.G., Burger, L., and Matthias, P. (2015). Enhancer repertoires are reshaped independently of early priming and heterochromatin dynamics during B cell differentiation. Nat. Commun. *6*, 8324.

Clemente-Casares, X., Blanco, J., Ambalavanan, P., Yamanouchi, J., Singha, S., Fandos, C., Tsai, S., Wang, J., Garabatos, N., Izquierdo, C., et al. (2016). Expanding antigen-specific regulatory networks to treat autoimmunity. Nature *530*, 434–440.

Daikoku, T., Tranguch, S., Friedman, D.B., Das, S.K., Smith, D.F., and Dey, S.K. (2005). Proteomic analysis identifies immunophilin FK506 binding protein 4 (FKBP52) as a downstream target of Hoxa10 in the periimplantation mouse uterus. Mol. Endocrinol. *19*, 683–697.

Deng, W., Cha, J., Yuan, J., Haraguchi, H., Bartos, A., Leishman, E., Viollet, B., Bradshaw, H.B., Hirota, Y., and Dey, S.K. (2016). p53 coordinates decidual sestrin 2/AMPK/mTORC1 signaling to govern parturition timing. J. Clin. Invest. *126*, 2941–2954.

Durant, L., Watford, W.T., Ramos, H.L., Laurence, A., Vahedi, G., Wei, L., Takahashi, H., Sun, H.W., Kanno, Y., Powrie, F., and O'Shea, J.J. (2010). Diverse targets of the transcription factor STAT3 contribute to T cell pathogenicity and homeostasis. Immunity *32*, 605–615.

Elovitz, M.A., and Mrinalini, C. (2004). Animal models of preterm birth. Trends Endocrinol. Metab. *15*, 479–487.

Fu, B., Zhou, Y., Ni, X., Tong, X., Xu, X., Dong, Z., Sun, R., Tian, Z., and Wei, H. (2017). Natural Killer Cells Promote Fetal Development through the Secretion of Growth-Promoting Factors. Immunity *47*, 1100–1113.e1106.

Goldenberg, R.L., Culhane, J.F., Iams, J.D., and Romero, R. (2008). Epidemiology and causes of preterm birth. Lancet *371*, 75–84.

Hierweger, A.M., Engler, J.B., Friese, M.A., Reichardt, H.M., Lydon, J., DeMayo, F., Mittrücker, H.W., and Arck, P.C. (2019). Progesterone modulates the T-cell response via glucocorticoid receptor-dependent pathways. Am. J. Reprod. Immunol. *81*, e13084.

Hirota, Y., Daikoku, T., Tranguch, S., Xie, H., Bradshaw, H.B., and Dey, S.K. (2010). Uterine-specific p53 deficiency confers premature uterine senescence and promotes preterm birth in mice. J. Clin. Invest. *120*, 803–815.

Hirota, Y., Cha, J., Yoshie, M., Daikoku, T., and Dey, S.K. (2011). Heightened uterine mammalian target of rapamycin complex 1 (mTORC1) signaling provokes preterm birth in mice. Proc. Natl. Acad. Sci. USA *108*, 18073–18078.

Hoshino, K., Takeuchi, O., Kawai, T., Sanjo, H., Ogawa, T., Takeda, Y., Takeda, K., and Akira, S. (1999). Cutting edge: Toll-like receptor 4 (TLR4)-deficient mice are hyporesponsive to lipopolysaccharide: evidence for TLR4 as the Lps gene product. J. Immunol. *162*, 3749–3752.

Ip, W.K.E., Hoshi, N., Shouval, D.S., Snapper, S., and Medzhitov, R. (2017). Anti-inflammatory effect of IL-10 mediated by metabolic reprogramming of macrophages. Science *356*, 513–519.

Johnson, D.E., O'Keefe, R.A., and Grandis, J.R. (2018). Targeting the IL-6/JAK/STAT3 signalling axis in cancer. Nat. Rev. Clin. Oncol. *15*, 234–248.

Kadam, L., Gomez-Lopez, N., Mial, T.N., Kohan-Ghadr, H.R., and Drewlo, S. (2017). Rosiglitazone Regulates TLR4 and Rescues HO-1 and NRF2 Expression in Myometrial and Decidual Macrophages in Inflammation-Induced Preterm Birth. Reprod. Sci. *24*, 1590–1599.

Kim, D., Pertea, G., Trapnell, C., Pimentel, H., Kelley, R., and Salzberg, S.L. (2013). TopHat2: accurate alignment of transcriptomes in the presence of insertions, deletions and gene fusions. Genome Biol. *14*, R36.

Kisanuki, Y.Y., Hammer, R.E., Miyazaki, J., Williams, S.C., Richardson, J.A., and Yanagisawa, M. (2001). Tie2-Cre transgenic mice: a new model for endothelial cell-lineage analysis in vivo. Dev. Biol. *230*, 230–242.

Kortylewski, M., Xin, H., Kujawski, M., Lee, H., Liu, Y., Harris, T., Drake, C., Pardoll, D., and Yu, H. (2009). Regulation of the IL-23 and IL-12 balance by Stat3 signaling in the tumor microenvironment. Cancer Cell *15*, 114–123.

Kühn, R., Löhler, J., Rennick, D., Rajewsky, K., and Müller, W. (1993). Interleukin-10-deficient mice develop chronic enterocolitis. Cell *75*, 263–274.

Langmead, B., and Salzberg, S.L. (2012). Fast gapped-read alignment with Bowtie 2. Nat. Methods *9*, 357–359.

Lui, S., Duval, C., Farrokhnia, F., Girard, S., Harris, L.K., Tower, C.L., Stevens, A., and Jones, R.L. (2018). Delineating differential regulatory signatures of the human transcriptome in the choriodecidua and myometrium at term labor. Biol. Reprod. *98*, 422–436.

Manzanillo, P., Eidenschenk, C., and Ouyang, W. (2015). Deciphering the crosstalk among IL-1 and IL-10 family cytokines in intestinal immunity. Trends Immunol. *36*, 471–478.

McAlees, J.W., Whitehead, G.S., Harley, I.T., Cappelletti, M., Rewerts, C.L., Holdcroft, A.M., Divanovic, S., Wills-Karp, M., Finkelman, F.D., Karp, C.L., and Cook, D.N. (2015). Distinct Tlr4-expressing cell compartments control neutrophilic and eosinophilic airway inflammation. Mucosal Immunol. *8*, 863–873.

Miller, S.I., Ernst, R.K., and Bader, M.W. (2005). LPS, TLR4 and infectious disease diversity. Nat. Rev. Microbiol. *3*, 36–46.

Moffett, A., and Loke, C. (2006). Immunology of placentation in eutherian mammals. Nat. Rev. Immunol. *6*, 584–594.

Moster, D., Lie, R.T., and Markestad, T. (2008). Long-term medical and social consequences of preterm birth. N. Engl. J. Med. *359*, 262–273.

Nancy, P., Tagliani, E., Tay, C.S., Asp, P., Levy, D.E., and Erlebacher, A. (2012). Chemokine gene silencing in decidual stromal cells limits T cell access to the maternal-fetal interface. Science *336*, 1317–1321.

Nancy, P., Siewiera, J., Rizzuto, G., Tagliani, E., Osokine, I., Manandhar, P., Dolgalev, I., Clementi, C., Tsirigos, A., and Erlebacher, A. (2018). H3K27me3 dynamics dictate evolving uterine states in pregnancy and parturition. J. Clin. Invest. *128*, 233–247.

Robertson, S.A., Christiaens, I., Dorian, C.L., Zaragoza, D.B., Care, A.S., Banks, A.M., and Olson, D.M. (2010). Interleukin-6 is an essential determinant of on-time parturition in the mouse. Endocrinology *151*, 3996–4006.

Robertson, S.A., Wahid, H.H., Chin, P.Y., Hutchinson, M.R., Moldenhauer, L.M., and Keelan, J.A. (2018). Toll-like Receptor-4: A New Target for Preterm Labour Pharmacotherapies? Curr. Pharm. Des. *24*, 960–973.

Romero, R., Dey, S.K., and Fisher, S.J. (2014). Preterm labor: one syndrome, many causes. Science *345*, 760–765.

Rubens, C.E., Sadovsky, Y., Muglia, L., Gravett, M.G., Lackritz, E., and Gravett, C. (2014). Prevention of preterm birth: harnessing science to address the global epidemic. Sci. Transl. Med. *6*, 262sr5.

Saraiva, M., and O'Garra, A. (2010). The regulation of IL-10 production by immune cells. Nat. Rev. Immunol. *10*, 170–181.

Soyal, S.M., Mukherjee, A., Lee, K.Y., Li, J., Li, H., DeMayo, F.J., and Lydon, J.P. (2005). Cre-mediated recombination in cell lineages that express the progesterone receptor. Genesis *41*, 58–66.

Suryawanshi, H., Morozov, P., Straus, A., Sahasrabudhe, N., Max, K.E.A., Garzia, A., Kustagi, M., Tuschl, T., and Williams, Z. (2018). A single-cell survey of the human first-trimester placenta and decidua. Sci. Adv. *4*, eaau4788.

Tachi, C., and Tachi, S. (1986). Macrophages and implantation. Ann. N Y Acad. Sci. *476*, 158–182.

Takeda, K., Clausen, B.E., Kaisho, T., Tsujimura, T., Terada, N., Förster, I., and Akira, S. (1999). Enhanced Th1 activity and development of chronic enterocolitis in mice devoid of Stat3 in macrophages and neutrophils. Immunity *10*, 39–49.

Tang, A.T., Choi, J.P., Kotzin, J.J., Yang, Y., Hong, C.C., Hobson, N., Girard, R., Zeineddine, H.A., Lightle, R., Moore, T., et al. (2017). Endothelial TLR4 and the microbiome drive cerebral cavernous malformations. Nature *545*, 305–310.

Vento-Tormo, R., Efremova, M., Botting, R.A., Turco, M.Y., Vento-Tormo, M., Meyer, K.B., Park, J.E., Stephenson, E., Polański, K., Goncalves, A., et al. (2018). Single-cell reconstruction of the early maternal-fetal interface in humans. Nature *563*, 347–353.

Wahid, H.H., Dorian, C.L., Chin, P.Y., Hutchinson, M.R., Rice, K.C., Olson, D.M., Moldenhauer, L.M., and Robertson, S.A. (2015). Toll-Like Receptor 4 Is an Essential Upstream Regulator of On-Time Parturition and Perinatal Viability in Mice. Endocrinology *156*, 3828–3841.

Yan, H., Li, H., Zhu, L., Gao, J., Li, P., and Zhang, Z. (2018). Increased TLR4 and TREM-1 expression on monocytes and neutrophils in preterm birth: further evidence of a proinflammatory state. J. Matern. Fetal Neonatal Med. *25*, 1–9.

Yasukawa, H., Ohishi, M., Mori, H., Murakami, M., Chinen, T., Aki, D., Hanada, T., Takeda, K., Akira, S., Hoshijima, M., et al. (2003). IL-6 induces an anti-inflammatory response in the absence of SOCS3 in macrophages. Nat. Immunol. *4*, 551–556.

Yazji, I., Sodhi, C.P., Lee, E.K., Good, M., Egan, C.E., Afrazi, A., Neal, M.D., Jia, H., Lin, J., Ma, C., et al. (2013). Endothelial TLR4 activation impairs intestinal microcirculatory perfusion in necrotizing enterocolitis via eNOS-NO-nitrite signaling. Proc. Natl. Acad. Sci. USA *110*, 9451–9456.

Yuan, J., Cha, J., Deng, W., Bartos, A., Sun, X., Ho, H.H., Borg, J.P., Yamaguchi, T.P., Yang, Y., and Dey, S.K. (2016). Planar cell polarity signaling in the uterus directs appropriate positioning of the crypt for embryo implantation. Proc. Natl. Acad. Sci. USA *113*, E8079–E8088.

Yuan, J., Deng, W., Cha, J., Sun, X., Borg, J.P., and Dey, S.K. (2018). Tridimensional visualization reveals direct communication between the embryo and glands critical for implantation. Nat. Commun. *9*, 603.

Zanoni, I., Ostuni, R., Marek, L.R., Barresi, S., Barbalat, R., Barton, G.M., Granucci, F., and Kagan, J.C. (2011). CD14 controls the LPS-induced endocytosis of Toll-like receptor 4. Cell *147*, 868–880.

Zhang, Y., Liu, T., Meyer, C.A., Eeckhoute, J., Johnson, D.S., Bernstein, B.E., Nusbaum, C., Myers, R.M., Brown, M., Li, W., and Liu, X.S. (2008). Model-based analysis of ChIP-Seq (MACS). Genome Biol. *9*, R137.

STAR★METHODS

KEY RESOURCES TABLE

REAGENT or RESOURCE	SOURCE	IDENTIFIER
Antibodies		
Rat anti-CD31	BD Biosciences	Cat# 553370; RRID:AB_563954
Rabbit anti-PR	Cell Signaling	Cat# 8757s; RRID:AB_2797144
Rabbit anti-pStat3	Cell Signaling	Cat# 9145s; RRID:AB_2491009
Rabbit anti-NFκB	Cell Signaling	Cat# 8242s; RRID:AB_10859369
Rabbit anti-pNFκB	Cell Signaling	Cat# 3031s; RRID:AB_330559
Rabbit anti-Cox2	Cell Signaling	Cat# 12282s; RRID:AB_2571729
Rabbit anti-H3K4me3	Cell Signaling	Cat# 9751s; RRID:AB_2616028
Rabbit anti-pS6	Cell Signaling	Cat# 2211s; RRID:AB_331679
Rabbit anti-S6	Cell Signaling	Cat# 2217s; RRID:AB_331355
Rabbit anti-Tubulin	Cell Signaling	Cat# 2144s; RRID:AB_2210548
Rabbit anti-Lamin A/C	Cell Signaling	Cat# 2032s; RRID:AB_10694918
Rabbit anti-TLR4	Cell Signaling	Cat# 14358s; RRID:AB_2798460
Rat anti-CD4 (RM4-5)	Biolegend	Cat# 100505; RRID:AB_312708
Rat Anti-CD45	Biolegend	Cat# 103102; RRID:AB_312967
Rat Anti-Ly6G	BD Bioscience	Cat# 551459; RRID:AB_394206
Rat Anti-F4/80	Bio-Rad	Cat# MCA497R; RRID:AB_323279
Fluorescein labeled Dolichos Biflorus Agglutinin (DBA)	Vectorlabs	Cat# FL-1031-2
Cy3 AffiniPure Donkey Anti-Rat IgG (H+L)	Jackson ImmunoResearch	Cat# 712-165-150; RRID:AB_2340666
Cy3 AffiniPure Donkey Anti-Goat IgG (H+L)	Jackson ImmunoResearch	Cat# 705-165-147; RRID:AB_2307351
Alexa Fluor® 594 AffiniPure Donkey Anti-Rabbit IgG (H+L)	Jackson ImmunoResearch	Cat# 711-585-152; RRID:AB_2340621
Alexa Fluor® 488 AffiniPure Donkey Anti-Rabbit IgG (H+L)	Jackson ImmunoResearch	Cat# 711-545-152; RRID:AB_2313584
Cy2 AffiniPure Donkey Anti-Rat IgG (H+L)	Jackson ImmunoResearch	Cat# 712-225-153; RRID:AB_2340674
Chemicals, Peptides, and Recombinant Proteins		
LPS	Invivogen	Cat# tlrl-3pelps
rIL6	Peprotech	Cat# 216-16
BSA	Thermo Scientific	Cat# AM2616
Hoechst 33342	Thermo Scientific	Cat# H1399
Anti-IL10	Custom made	N/A
Deposited Data		
Day 4 uterus RNA-Seq data	This study	GEO: GSE116096
Day 8 and 16 stromal cells RNA-Seq data	Nancy et al., 2018	SRA: SRP120624
Stat3 ChIP-Seq	Durant et al., 2010	SRA: SRX020337
H3K4me3 ChIP-Seq	Choukrallah et al., 2015	SRA: SRX668829
Experimental Models: Organisms/Strains		
Mouse: *Tlr4*$^{f/f}$	McAlees et al., 2015	N/A
Mouse: *p53*$^{f/f}$	Hirota et al., 2010	N/A
Mouse: *Pgr*$^{Cre/+}$	Soyal et al., 2005	N/A
Mouse: *Tie2*$^{Cre/+}$	Kisanuki et al., 2001	N/A
Mouse: *Tlr4*$^{-/-}$	Hoshino et al., 1999	N/A
Software and Algorithms		
Bowtie2	Langmead and Salzberg, 2012	http://bowtie-bio.sourceforge.net/bowtie2/index.shtml
MACS2	Zhang et al., 2008	https://github.com/taoliu/MACS

(*Continued on next page*)

Continued

REAGENT or RESOURCE	SOURCE	IDENTIFIER
TopHat2	Kim et al., 2013	https://ccb.jhu.edu/software/tophat/index.shtml
GraphPad Prism	GraphPad	https://www.graphpad.com/scientific-software/prism/

CONTACT FOR REAGENT AND RESOURCE SHARING

Further information and requests for reagents may be directed to, and will be fulfilled by the Lead Contact S. K. Dey (SK.Dey@cchmc.org).

EXPERIMENTAL MODELS AND SUBJECT DETAILS

Animal care and housing

Pgr$^{Cre/+}$*Tlr4*$^{f/f}$ and *Tie2*$^{Cre/+}$*Tlr4*$^{f/f}$ female mice were generated by crossing *Tlr4* floxed (*Tlr4*$^{f/f}$, C57BL/6,129 mixed background) females with *Pgr*$^{Cre/+}$ and *Tie2*$^{Cre/+}$ males (C57BL/6,129 and albino B6 mixed background) (Kisanuki et al., 2001; Soyal et al., 2005). *Tie2*$^{Cre/+}$*Rosa26*^{tdTomato} mice were generated by crossing *Tie2*$^{cre/+}$ males with *Rosa26*^{tdTomato} female mice (Jackson lab). *Pgr*$^{Cre/+}$*p53*$^{f/f}$ mice were generated by crossing *p53* floxed mice (Hirota et al., 2010) with *Pgr*$^{Cre/+}$ males. *Tlr4* floxed mice have previously been described and were originally obtained from Chris Karp's group (McAlees et al., 2015). *Tlr4*$^{-/-}$ (C57BL/6,129 mixed background) mice have previously been described (Hoshino et al., 1999). At least three female mice from each genotype were used for individual experiments. All mice used in this study were housed in the Cincinnati Children's Hospital Medical Center Animal Care Facility according to NIH and institutional guidelines for the use of laboratory animals. All protocols of the present study were reviewed and approved by the Cincinnati Children's Hospital Research Foundation Institutional Animal Care and Use Committee. Mice were given autoclaved rodent LabDiet 5010 (Purina) and UV light–sterilized RO/DI constant circulation water *ad libitum* and were housed under a constant 12-hour light/12-hour dark cycle.

Cell cultures and treatments

Stromal cells from day 4 of WT pregnant mice were collected by enzymatic digestion as previously described (Deng et al., 2016). The purity of stromal was confirmed by Vimentin and Desmin staining according to our published study (Daikoku et al., 2005). Isolated stromal cells were decidualized by estradiol-17β (E_2, 10 nM) and progesterone (P_4, 1 μM) in phenol red–free DMEM/F12 media supplemented with charcoal-stripped 1% FBS (vol/vol) for 4 days and medium was changed every 2 days.

METHOD DETAILS

Analysis of pregnancy outcomes

Three adult females from each genotype were housed with floxed fertile males from respective backgrounds overnight in separate cages. Successful mating (day 1 of pregnancy) was defined as the morning of finding the presence of a vaginal plug. Plug-positive females were housed separately until processed for experiments. Litter size, pregnancy rate and outcomes were monitored in timed pregnant mice. Ultrapure TLR4-specific LPS (2.5 μg/mouse and 40 μg/mouse, InvivoGen) was administered intraperitoneally (i.p.) on day 16 of pregnancy. Parturition was monitored from days 16 through 21 by daily observation of mice in the morning, noon and evening. Birth timing was defined by the observation of the first pup born. PTB was defined as birth occurring earlier than day 19 of pregnancy (day 1 = vaginal plug in the morning). Resorption sites and placental scars were identified in dams showing preterm or difficult deliveries by examination of the uterus. The number of pups/masses delivered was compared with the number of resorption sites and placental scars. Anti-IL10 antibody (500 μg/mouse, i.p., custom made, JES5-2A5) (Clemente-Casares et al., 2016) was injected in both *p53*$^{f/f}$ and *Pgr*$^{Cre/+}$*p53*$^{f/f}$ mice 30 min before and after LPS injection (1 μg/mouse, i.p.). At least three independent mice in each genotype were used for biochemical and immunostaining assays.

Immunofluorescence (IF)

Frozen sections (12 μm) were fixed in 4% paraformaldehyde (PFA). After blocking in 5% BSA, sections were incubated with specific primary antibodies at 4°C overnight (Yuan et al., 2016). After incubation with first antibody, slides were incubated in secondary antibodies conjugated with Cy-2, Cy-3, Alexa 488 or Alexa 594 (1:300, Jackson Immuno Research). Nuclear staining was performed using Hoechst 33342 (1:500, H1399, Thermo Scientific).

RNA Isolation and qPCR

RNA from tissue or cells in TRIzol was extracted by chloroform and isopropanol. Up to 500ng total RNA after removing genomic DNA from each sample was reverse transcribed with cDNA kit, and quantitative RT-PCR was performed in ABI Thermal Cyclers Real-Time PCR machine by $2^{-\Delta\Delta CT}$ method (Yuan et al., 2018). *rpL7* served as an internal control and the relative expression was calculated according to manufacturer's protocol.

Immunoblotting

Samples were homogenized in RIPA buffer with protease and phosphatase inhibitors and quantified using a BCA kit. The protein extracts were run in 10% Bis-acrylamide gel and transferred to PVDF membranes. After blocking in 5% non-fat milk, the membranes were incubated with indicated antibodies overnight in 4°C. The membranes were washed in TBS-T and incubated with HRP conjugated secondary antibodies. The signal was visualized with an ECL kit.

Isolations of nuclei and cytoplasm

Deciduae from day 16 were collected and dissected from placenta, then subjected to homogenization by Dounce tissue grinder in PBS with proteinase and phosphatase inhibitors. After centrifuging, cells were resuspended in Buffer A (10 mM HEPES pH7.9, 10mM KCl, 0.1mM EDTA, 1mM DTT and 0.5mM PMSF, 2.5% NP40). Then the samples were centrifuged for 5 min at 15000 rpm. The supernatant was kept for cytoplasm and the remaining nuclei were dissolved in Buffer C (20 mM HEPES pH7.9, 400mM NaCl, 1mM EDTA, 1mM DTT and 1mM PMSF) by vibrating for 30 mins. Both cytoplasm and nuclei were normalized to the same concentrations of protein.

In situ hybridization

Paraformaldehyde-fixed frozen sections from control and experimental groups were processed onto poly-L-lysine-coated slides and hybridized in formamide buffer with specific ^{35}S-labeled cRNA probes. The slides were then coated with Carestream NTB emulsion and autoradiographs were developed and visualized under a Nikon dark-field microscope. Mouse-specific anti-sense cRNA probes for *Cox2*, *Il6*, *Tlr4 GzmA, GzmC, Il6r* and *Gp130* were used. For DIG-ISH, DIG-labeled probes were generated according to the manufacturer's protocol (Roche). After hybridization in formamide buffer, the slides were blocked in blocking buffer and incubated with Alkaline Phosphatase conjugated anti-Dig antibody and visualized by NBT/BCIP substrate (Yuan et al., 2016).

RNA-FISH

Fluorescence *in situ* hybridization was developed in our lab based on previously established DIG *in situ* hybridization (Yuan et al., 2016). In brief, following proteinase K (5 mg/ml) digestion and acetylation, slides were hybridized with DIG-labeled probes at 55°C. Anti-Dig-peroxidase was applied onto hybridized slides following washing and peroxide quenching. Color was developed by TSA (Tyramide signal amplification) Fluorescein according to the manufacturer's instructions (PerkinElmer).

ChIP-PCR Assays

Day 16 decidua tissues from vehicle and LPS treated group were homogenized by Dounce tissue grinder in cold PBS with proteinase and phosphatase inhibitors. After centrifuging, the decidual stromal cells were washed with PBS and fixed in 10 mL of PBS containing 1% formaldehyde, then terminated by adding 2.5 M glycine. After incubation in Mg-NI buffer (15 mM Tris-HCl, pH 7.5, 5 mM MgCl2, 60 mM KCl, 0.5 mM DTT, 15 mM NaCl, and 300 mM sucrose) and Mg-NI-Nonidet P-40 buffer (Mg-NI buffer with 1% Nonidet P-40), cell pellets were resuspended in lysis buffer (1% SDS, 50 mM Tris-HCl, pH 8.0, and 0.5 mM EDTA) and sonicated by repeating a program (15 s on and 30 s off at 45% amplitude) 8 times. After the samples were centrifuged at 13,000 rpm for 10 min to pellet cell debris, the soluble chromatin was harvested. Immunoprecipitation was performed by incubation with antibody coated magnet beads. After washing, DNA was eluted from the beads and subjected to Real-time PCR with specific primers.

Identification of whole-genome binding sites of Stat3 and H3K4me3

The datasets used in this study were from GSM540722 (Durant et al., 2010) and GSE60005 (Choukrallah et al., 2015). Sequenced reads were aligned to the mouse genome (mm9) by bowtie2 (Langmead and Salzberg, 2012). Only non-redundant reads that passed the quality score were kept for downstream analysis. MACS2 (Model-Based Analysis of ChIP-Seq)(Zhang et al., 2008) was used to identify the peaks. The peaks were visualized in IGV browser.

Expression status of Tlrs identified by RNA-Seq analysis

Day 4 stromal and epithelial cells were isolated by enzyme digestion and total mRNA were extracted by TRIzol (Yuan et al., 2018). Total rRNAs were removed by RiboZero and the remaining RNAs were sequenced by HiSeq2500. The RNA-seq results of reported decidualized mouse stromal cells from day 8 and day 16 (Nancy et al., 2018) were re-analyzed by Tophat2 (Kim et al., 2013) and visualized by R (GEO: GSE105456). The RNA-Seq data of human normal endometrium data was downloaded from TCGA (The Cancer Genome Atlas) Data Portal. The expression of TLR4 in human endometrium cells was represented by RSEM (RNA-Seq by Expectation-Maximization) and visualized by R.

QUANTIFICATION AND STATISTICAL ANALYSIS

Each experiment was repeated several times depending on the consistency of the results. Statistical analyses were performed using two-tailed Student's t test and ANOVA. Shapiro-Wilk test was applied for normality test. A value of $p < 0.05$ was considered statistically significant.

DATA AND SOFTWARE AVAILABILITY

All data are available in the main text or the supplementary materials. RNA-seq data of day 4 epithelium and stroma have been deposited in the Gene Expression Omnibus under accession number GEO: GSE116096.

Cell Reports, Volume *27*

Supplemental Information

Endothelial Cells in the Decidual Bed Are Potential Therapeutic Targets for Preterm Birth Prevention

Wenbo Deng, Jia Yuan, Jeeyeon Cha, Xiaofei Sun, Amanda Bartos, Hideo Yagita, Yasushi Hirota, and Sudhansu K. Dey

Supplemental Information

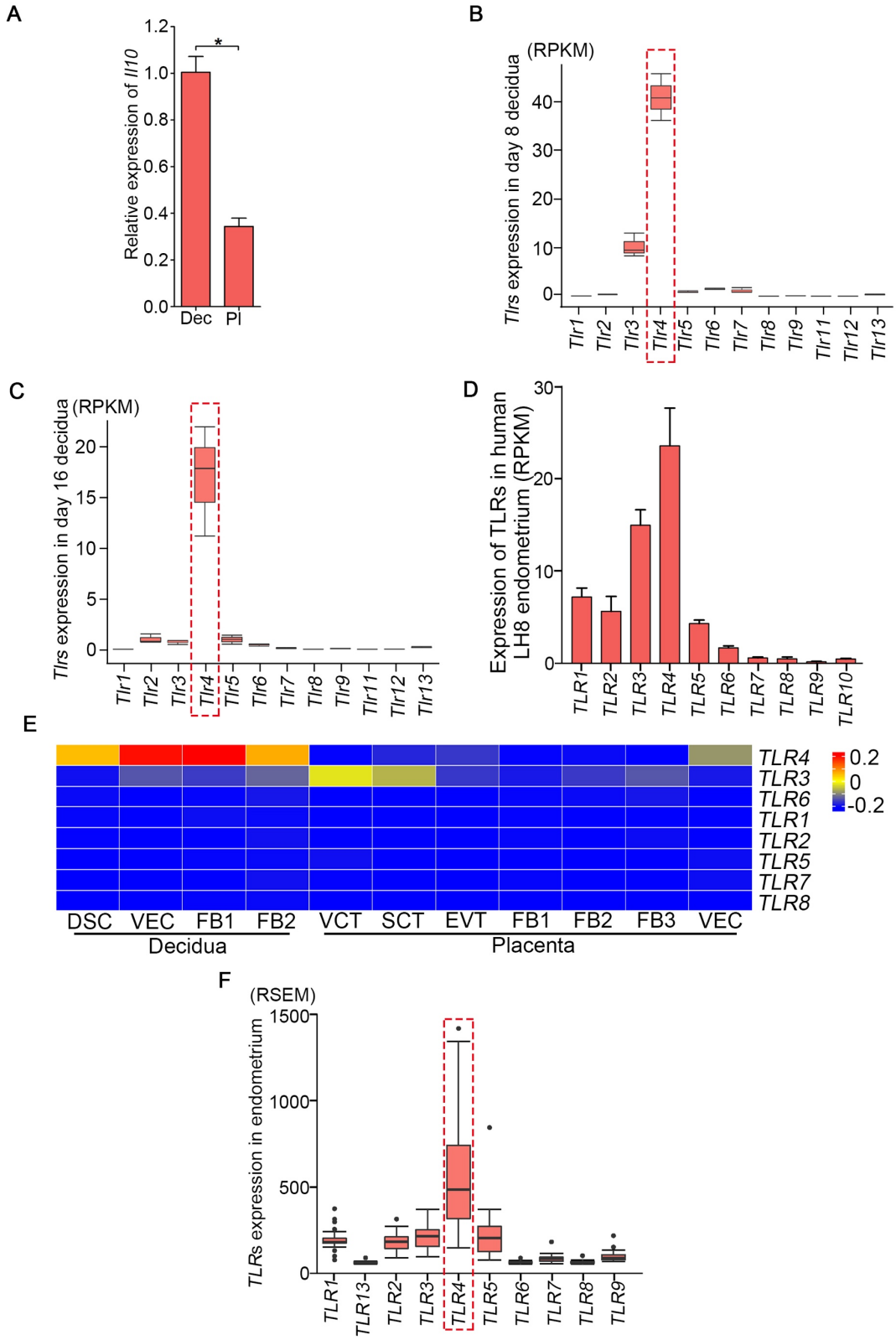

Figure S1, related to Figure 1. TLR4 is the dominant member expressed in the decidua during pregnancy

(A) Relative expression of *Il10* in day 16 decidua (Dec) and placenta (Pl). n=3, *p<0.05. Data are represented as mean ± SEM.

(B and C) Relative expression of the members of *Tlr* family in isolated stromal cells from days 8 and 16 and recalculated from published database. RPKM: reads per kilobase per million.

(D) Expression of *TLR* family in LH8 human endometrium. RPKM: reads per kilobase per million.

(E) Expression of *TLR* family in different cell types from single-cell sequencing in first trimester decidua and placenta. DSC: decidual stromal cells; VEC: vascular endothelial cells; FB: fibroblast cells; VCT: villous cytotrophoblasts; SCT: syncytiotrophoblasts; EVT: extravillous trophoblasts

(F) Expression of all *TLR* members in normal human endometrium from human TCGA database. RSEM: RNA-Seq by Expectation-Maximization.

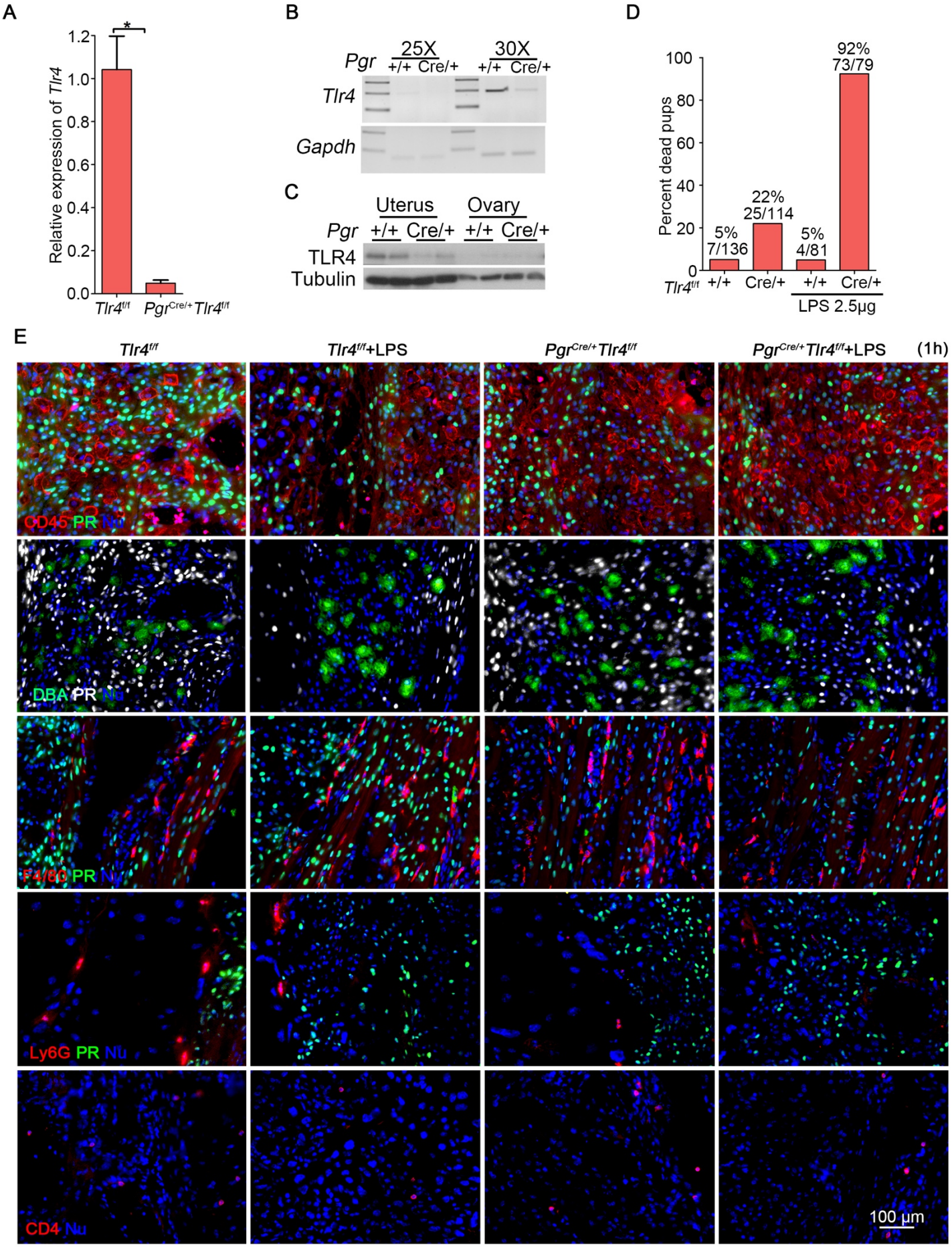
A
Relative expression of Tlr4
1.2
1.0
0.8
0.6
0.4
0.2
0.0
*
Tlr4f/f
PgrCre/+Tlr4f/f
B
Pgr
25X
30X
+/+ Cre/+ +/+ Cre/+
Tlr4
Gapdh
C
Uterus
Ovary
Pgr
+/+ Cre/+ +/+ Cre/+
TLR4
Tubulin
D
Percent dead pups
100
80
60
40
20
0
5%
7/136
22%
25/114
5%
4/81
92%
73/79
Tlr4f/f
+/+
Cre/+
+/+
Cre/+
LPS 2.5µg
E
Tlr4f/f
Tlr4f/f+LPS
PgrCre/+Tlr4f/f
PgrCre/+Tlr4f/f+LPS
(1h)
CD45 PR Nu
DBA PR Nu
F4/80 PR Nu
Ly6G PR Nu
CD4 Nu
100 µm

Figure S2, related to Figure 2. TLR4 deletion in uterus by Pgr-Cre

(A) Real-Time qPCR of *Tlr4* expression in *Tlr4*$^{f/f}$ and *Pgr*$^{Cre/+}$*Tlr4*$^{f/f}$ mice in uterus.

(B) RT-PCR of *Tlr4* expression in *Tlr4*$^{f/f}$ and *Pgr*$^{Cre/+}$*Tlr4*$^{f/f}$ mice at 25 and 30 cycles. *Gapdh* was used as an internal control.

(C) Western blotting of TLR4 in the uterus and ovary from *Tlr4*$^{f/f}$ and *Pgr*$^{Cre/+}$*Tlr4*$^{f/f}$ mice on day 8 of pregnancy.

(D) The ratio of dead pups to total number of pups/gestations in *Tlr4*$^{f/f}$ and *Pgr*$^{Cre/+}$*Tlr4*$^{f/f}$ mice in the presence or absence of low dose LPS (2.5 μg/mouse).

(E) Staining of CD45, DBA-lectin (uNK cells), F4/80, Ly6G, CD4 and PR in day 16 deciduae with or without LPS exposure for 1h. Scale bar, 100 μm

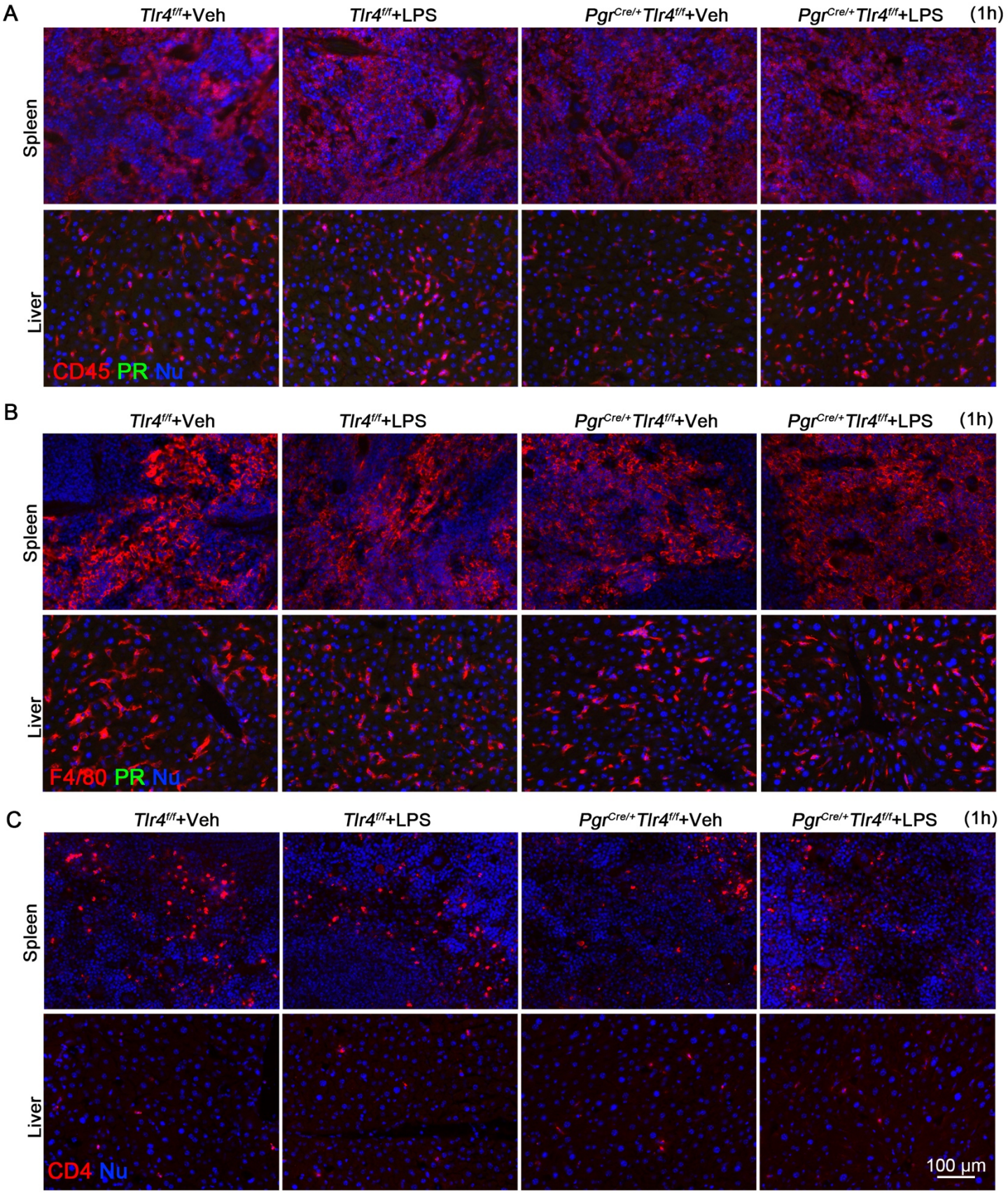
A
Tlr4f/f+Veh
Tlr4f/f+LPS
PgrCre/+Tlr4f/f+Veh
PgrCre/+Tlr4f/f+LPS
(1h)
Spleen
Liver
CD45 PR Nu
B
Tlr4f/f+Veh
Tlr4f/f+LPS
PgrCre/+Tlr4f/f+Veh
PgrCre/+Tlr4f/f+LPS
(1h)
Spleen
Liver
F4/80 PR Nu
C
Tlr4f/f+Veh
Tlr4f/f+LPS
PgrCre/+Tlr4f/f+Veh
PgrCre/+Tlr4f/f+LPS
(1h)
Spleen
Liver
CD4 Nu
100 μm

Figure S3, related to Figure 2. Expression of PR and CD45, F4/80 in the spleen and liver sections after LPS treatment in *Tlr4*$^{f/f}$ and *Pgr*$^{Cre/+}$*Tlr4*$^{f/f}$ deciduae

(A) Co-staining of CD45 and PR in *Tlr4*$^{f/f}$ and *Pgr*$^{Cre/+}$*Tlr4*$^{f/f}$ spleen and liver with or without LPS exposure.

(B) Co-staining of F4/80 and PR in *Tlr4*$^{f/f}$ and *Pgr*$^{Cre/+}$*Tlr4*$^{f/f}$ spleen and liver with or without LPS exposure.

(C) Co-staining of CD4 and PR in *Tlr4*$^{f/f}$ and *Pgr*$^{Cre/+}$*Tlr4*$^{f/f}$ spleen and liver with or without LPS treatment.

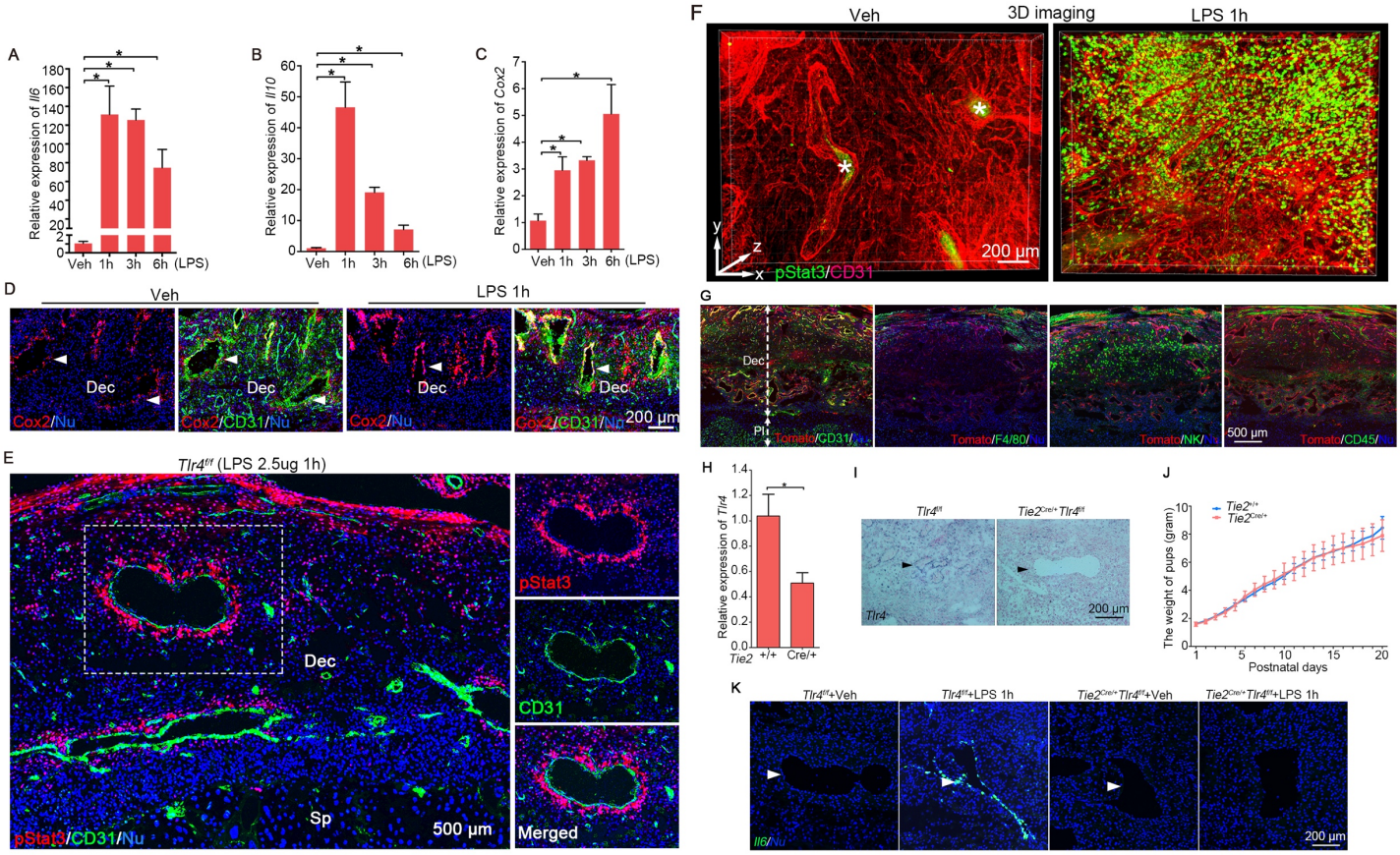
A
Relative expression of Il6
Veh 1h 3h 6h (LPS)
B
Relative expression of Il10
Veh 1h 3h 6h (LPS)
C
Relative expression of Cox2
Veh 1h 3h 6h (LPS)
D
Veh
LPS 1h
Dec
Cox2/Nu
Cox2/CD31/Nu
200 μm
E
Tlr4f/f (LPS 2.5ug 1h)
Dec
Sp
pStat3/CD31/Nu
500 μm
pStat3
CD31
Merged
F
Veh
3D imaging
LPS 1h
200 μm
pStat3/CD31
G
Dec
Pl
Tomato/CD31/Nu
Tomato/F4/80/Nu
Tomato/NK/Nu
500 μm
Tomato/CD45/Nu
H
Relative expression of Tlr4
Tie2 +/+ Cre/+
I
Tlr4f/f
Tie2Cre/+Tlr4f/f
Tlr4-
200 μm
J
Tie2+/+
Tie2Cre/+
The weight of pups (gram)
Postnatal days
K
Tlr4f/f+Veh
Tlr4f/f+LPS 1h
Tie2Cre/+Tlr4f/f+Veh
Tie2Cre/+Tlr4f/f+LPS 1h
Il6/Nu
200 μm

Figure S4, related to Figure 2 and 3. LPS induces cytokines in the decidua

(A-C) Relative expression of *Il6* (A), *Il10* (B) and *Cox2* (C), respectively, in *Tlr4*$^{f/f}$ mice after treatment with LPS for 1, 3 and 6 hours, n = 4, *, p<0.05. Data are represented as mean ± SEM.

(D) Co-immunostaining of Cox2 (red) and CD31 (green) in *p53*$^{f/f}$ deciduae after LPS treatment for 1 h. Dec: decidua. Arrowheads indicate endothelial cells. Scale bar, 200 μm.

(E) Co-immunofluorescence staining of pStat3 (red) and CD31 (green) in LPS-treated deciduae of *p53*$^{f/f}$ mice. Images in the right panels depict the images in the demarcated rectangles. Scale bar, 500 μm. Dec, deciduae; Sp, spongiotrophoblast.

(F) 3D Co-immunofluorescence staining of pStat3 (red) and CD31 (green) in the LPS-treated decidua in *p53*$^{f/f}$ mice. Scale bar, 100 μm.

(G) Staining of immune cells and endothelial cells markers in *Tie2*$^{Cre/+}$*Rosa*^{Tomato} reporter mice. Dec: decidua, Pl: placenta, Scale bar, 500 μm.

(H) Relative expression of *Tlr4* in day 16 deciduae in *Tlr4*$^{f/f}$ and *Tie2*$^{Cre/+}$*Tlr4*$^{f/f}$ mice. n=4, *, p<0.05. Data are represented as mean ± SEM.

(I) DIG-In situ hybridization of *Tlr4* in *Tlr4*$^{f/f}$ and *Tie2*$^{Cre/+}$*Tlr4*$^{f/f}$ mice. Arrow heads depict the location of endothelial cells. Scale bar, 200 μm.

(J) The weight of pups (gram) from days 1 to 20 after parturition between *Tlr4*$^{f/f}$ and *Tie2*$^{Cre/+}$*Tlr4*$^{f/f}$ mice (n=5).

(K) LPS-induced expression of *Il6* by fluorescence *in situ* hybridization in the endothelial cells in day 16 deciduae in *Tlr4*$^{f/f}$ and *Tie2*$^{Cre/+}$*Tlr4*$^{f/f}$ mice. Arrow heads indicate endothelial cells. Scale bar, 200 μm.

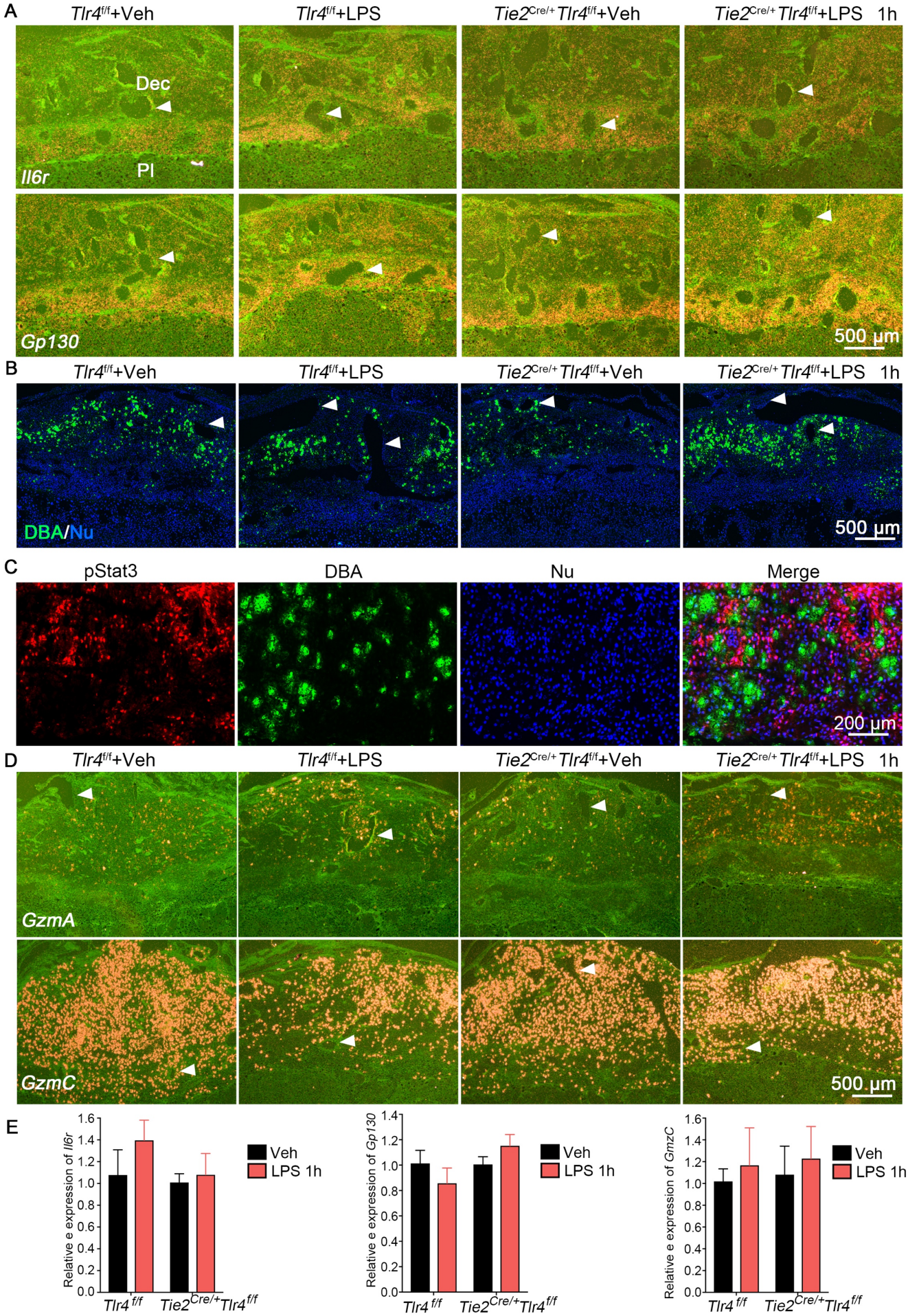
A
Tlr4f/f+Veh
Tlr4f/f+LPS
Tie2Cre/+Tlr4f/f+Veh
Tie2Cre/+Tlr4f/f+LPS 1h
Dec
Pl
Il6r
Gp130
500 μm
B
Tlr4f/f+Veh
Tlr4f/f+LPS
Tie2Cre/+Tlr4f/f+Veh
Tie2Cre/+Tlr4f/f+LPS 1h
DBA/Nu
500 μm
C
pStat3
DBA
Nu
Merge
200 μm
D
Tlr4f/f+Veh
Tlr4f/f+LPS
Tie2Cre/+Tlr4f/f+Veh
Tie2Cre/+Tlr4f/f+LPS 1h
GzmA
GzmC
500 μm
E
Relative e expression of Il6r
Relative e expression of Gp130
Relative e expression of GmzC
Veh
LPS 1h
Tlr4 f/f
Tie2Cre/+Tlr4f/f

Figure S5, related to Figure 4. In situ hybridization of *Il6*, *Gp130* and granzymes and co-staining of pStat3 and DAB-lectin in day 16 *Tlr4*$^{f/f}$ and *Tie2*$^{Cre/+}$*Tlr4*$^{f/f}$ deciduae.

(A) In situ hybridization for *Il6r* and *Gp130* in *Tlr4*$^{f/f}$ and *Tie2*$^{Cre/+}$*Tlr4*$^{f/f}$ decidua on day 16 after LPS (40 µg /mouse) treatment. Dec, decidua; Pl, Placenta. Scale bar, 500 µm.

(B) Immunolocalization of DBA+ NK cells (green) in *Tlr4*$^{f/f}$ and *Tie2*$^{Cre/+}$*Tlr4*$^{f/f}$ deciduae on day 16 in the absence or presence of LPS (40 µg /mouse) treatment. Scale bar, 500 µm.

(C) Co-immunolocalization of pStat3 (red) and DBA+ NK cells (green) in *Tlr4*$^{f/f}$ deciduae on day 16 after LPS (40 µg /mouse) treatment. Scale bar, 200 µm.

(D) In situ hybridization for *GzmA* and *GzmC* in *Tlr4*$^{f/f}$ and *Tie2*$^{Cre/+}$*Tlr4*$^{f/f}$ deciduae on day 16 after LPS (40 µg /mouse) treatment. Scale bar, 500 µm.

(E) Quantification of *Il6r, Gp130* and *GzmC* in *Tlr4*$^{f/f}$ and *Tie2*$^{Cre/+}$*Tlr4*$^{f/f}$ deciduae on day 16 after LPS (40 µg /mouse) treatment (n = 4). Relative expression is normalized against *rpL7* (a house-keeping gene).

Arrow heads indicate blood vessels in all images.

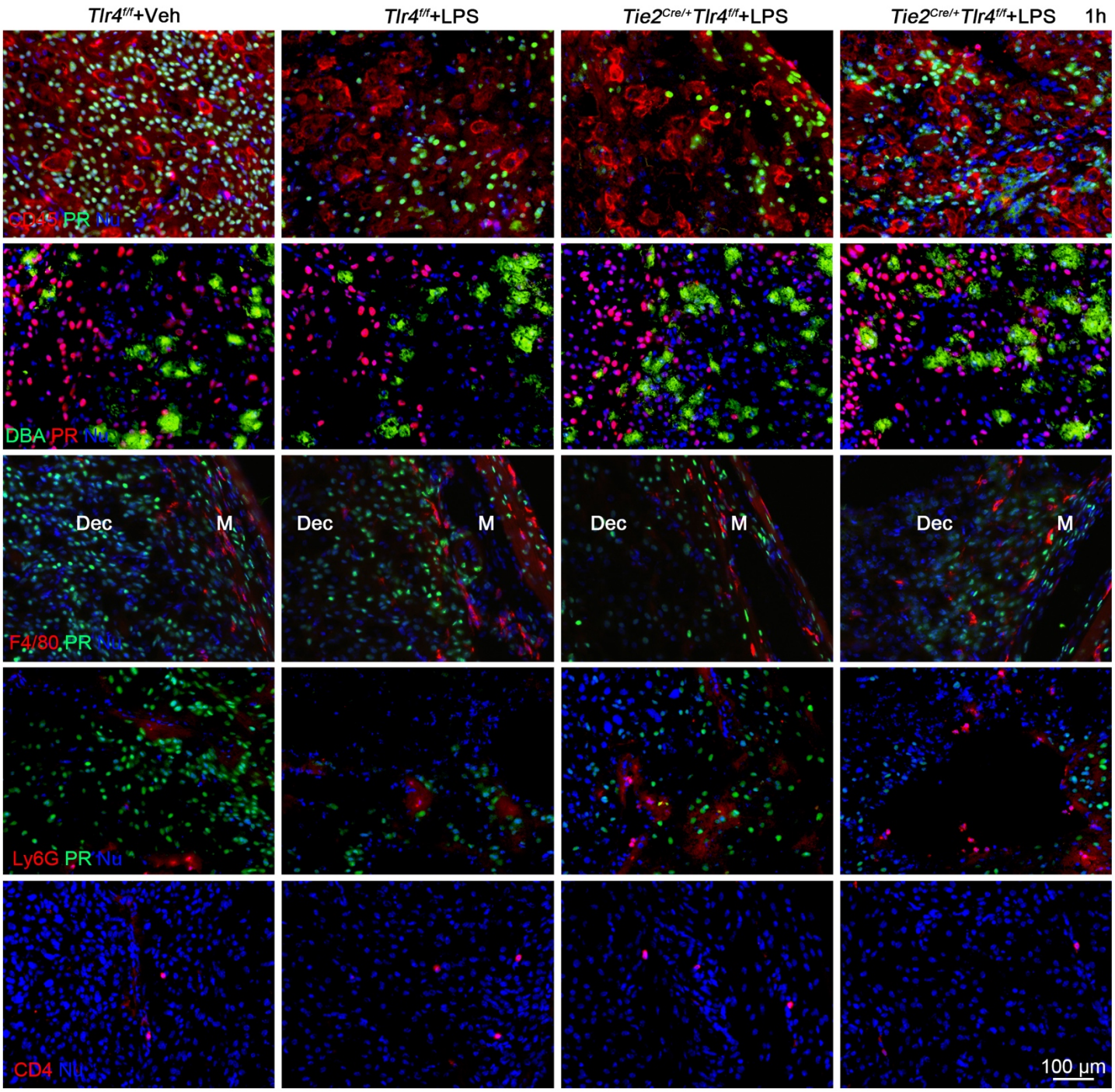
Tlr4f/f+Veh
Tlr4f/f+LPS
Tie2Cre/+Tlr4f/f+LPS
Tie2Cre/+Tlr4f/f+LPS
1h
CD45 PR Nu
DBA PR Nu
Dec
M
F4/80 PR Nu
Ly6G PR Nu
CD4 Nu
100 μm

Figure S6, related to Figure 4. Distribution of immune cell identified by specific marker in *Tlr4*$^{f/f}$ and *Tie2*$^{Cre/+}$*Tlr4*$^{f/f}$ deciduae after 1 hour of LPS treatment.

Co-staining of CD45, DBA-lectin, CD4, Ly6G and F4/80 with PR in *Tlr4*$^{f/f}$ and *Tie2*$^{Cre/+}$*Tlr4*$^{f/f}$ deciduae on day 16 after LPS (40 μg /mouse) treatment for 1 hour. Dec, deciduae; M, myometrium. Scale bar for all images, 100 μm.

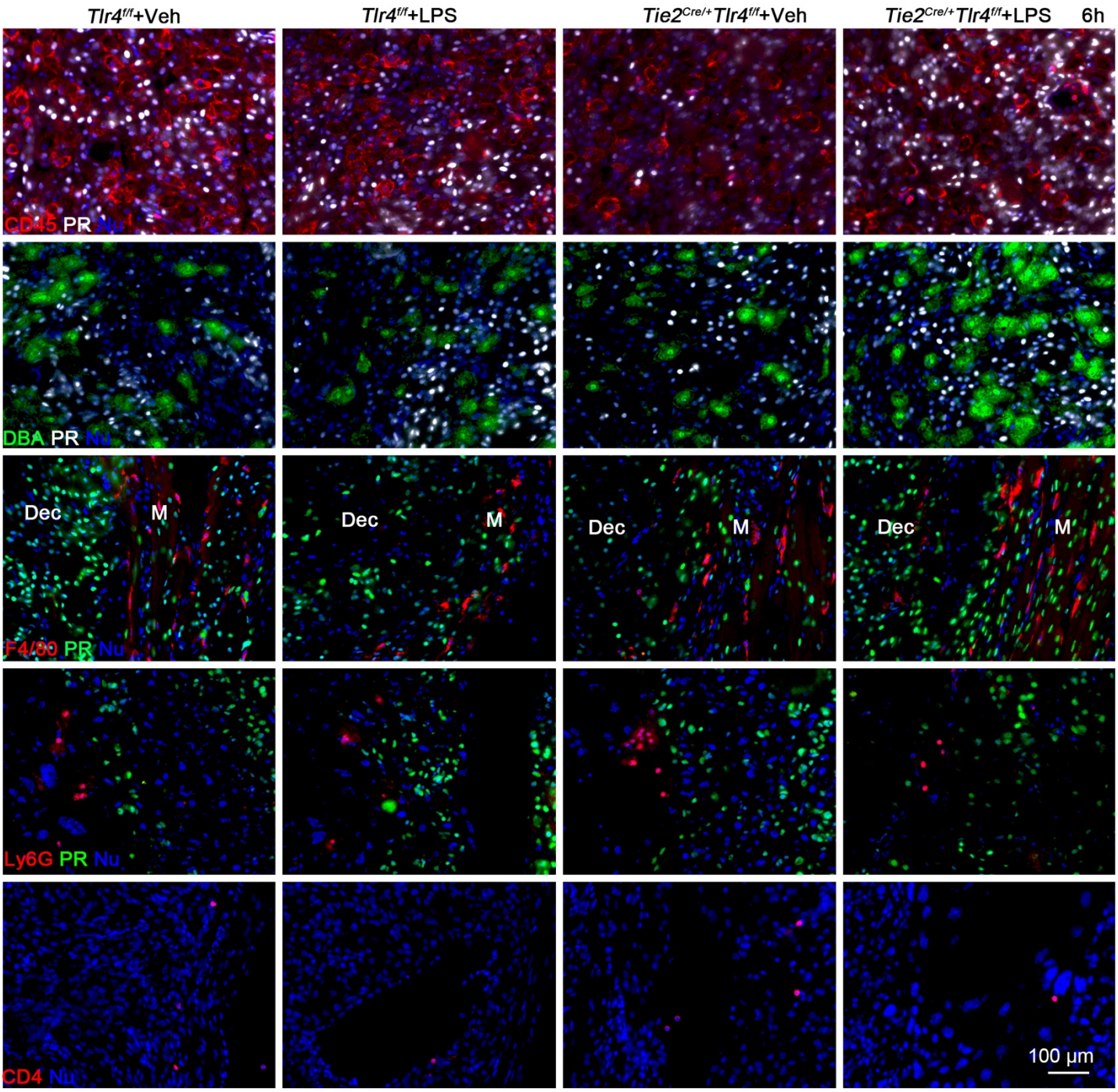
Tlr4f/f+Veh
Tlr4f/f+LPS
Tie2Cre/+Tlr4f/f+Veh
Tie2Cre/+Tlr4f/f+LPS
6h
CD45 PR Nu
DBA PR Nu
Dec
M
F4/80 PR Nu
Ly6G PR Nu
CD4 Nu
100 μm

Figure S7, related to Figure 4. Distribution of immune cell identified by specific marker in *Tlr4*$^{f/f}$ and *Tie2*$^{Cre/+}$*Tlr4*$^{f/f}$ deciduae after 6 hours of LPS treatment.

Co-staining of CD45, DBA-lectin, CD4, Ly6G and F4/80 with PR in *Tlr4*$^{f/f}$ and *Tie2*$^{Cre/+}$*Tlr4*$^{f/f}$ deciduae on day 16 after LPS (40 μg /mouse) treatment for 6 hours. Dec, deciduae; M, myometrium. Scale bar for all images, 100 μm.